Investigating human-landscape interaction three ways: reconstructing historical landslides, developing an educational program & quantifying mass export in Puerto Rico

A Dissertation Proposal by

Isabella Beatrice Bennett

May 2023

Committee:

Paul Bierman, Advisor

Jim Vigoreaux, Chair

Julia Perdrial

Amanda Schmidt

In partial fulfillment of the requirements for the degree of

Doctor of Philosophy in Natural Resources

Table of contents

1. ABSTRACT

Human environmental impacts create problems for present and future generations, both directly and indirectly. Mismanaged landscapes catalyze soil erosion, water pollution, and slope instability. As population grows and resource availability shrinks, these impacts magnify and compound. This is especially true of land use, as we have finite space on which to live, produce food, situate industry, store waste, and meet other human and ecological needs. My research sits at the intersection of earth surface processes, environmental justice, and education as I explore landscape change on geologic and human timescales. Using a multidisciplinary, systems-thinking approach, I evaluate human impacts on landscapes, for the purpose of better understanding and managing these resources.

I propose a dissertation that explores human-landscape interactions through three intersecting projects. 1) Using a Burlington, Vermont case study, I demonstrate how individual and governmental decisions over the past century led to a destabilized, landslide-prone slope, the repercussions of which are ongoing. This project explores the unforeseen consequences of land use and environmental resource modification, and underscores the importance of intentional and informed management. 2) Through the creation of an immersive environmental science education program, I examine the importance of undergraduate research exposure in efforts to improve diversity, access, and inclusion in STEM. 3) By quantifying rates of erosion in tropical Puerto Rico, both background and human-induced, I provide an example of how to better inform current and future land use and reduce impacts like soil loss and erosion. These projects contribute new insights for landscape management and broadening participation in STEM.

2. INTRODUCTION

My dissertation will include three distinct yet intersecting research projects, all centered around the common theme of human-landscape interaction (Figure 1). The field of human-landscape interactions recognizes that human systems are within and integrated into environmental systems (Stern, 1993). This field is transdisciplinary in nature and draws on physical, human, and biological sciences to identify and quantify the effects of human actions within the environmental system to better conceptualize and manage landscape change (Harden et al., 2014). I use methods and concepts from environmental science, geomorphology, geochemistry, education, historical studies, and diversity, equity, access, and inclusion research, to approach each of the three research projects that make up this dissertation. Aside from addressing the research goals described in the project descriptions below, my overarching goal is to ensure that the work I do is societally relevant and accessible - centering the broader impacts on the people and places involved and/or potentially affected by this work, and making the results appropriately available.

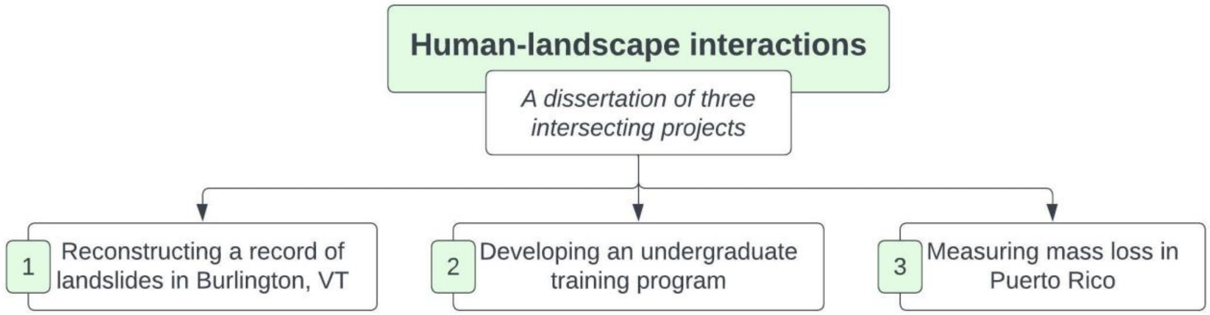

Figure 1*: The three projects that form my dissertation.*

My intended doctoral research project was to quantify erosion rates in eastern Cuba. Due to complications related to Covid-19 and political circumstances, it has not yet been possible for me to travel to Cuba for field work to start this project. In response, I have reevaluated and restructured my research into three projects related to different aspects of my interest in human-landscape interactions. These projects have thus far provided a wide breadth of learning and professional development experiences. This proposal is organized to describe each project in order of completion (Figure 1). I have completed project one and submitted a manuscript for review. Project two will be complete and documented this fall, following participant interviews and response analysis. Project three is the focus of my final year of doctoral research. Below, I briefly describe the background and relevant literature, methods, (preliminary) results, and, if applicable, ongoing work for each of these projects.

2.1 <u>Research significance:</u> The three projects of my dissertation will contribute to several areas of active and important research involving direct human impacts on landscapes.

- I expect that my findings regarding landslides in Burlington, Vermont, (chapter 1) will be considered in future slope management decisions made by the city of Burlington. This research could influence decisions that reduce the likelihood of future landslides, such as reforesting the slope and making a park, which would both reduce risk and create a safe green space for the community to use and enjoy.
- The undergraduate education program I developed (chapter 2) contributes to the growing body of literature regarding intentional models for increasing diversity, equity, inclusion, and belonging in STEM (Howard, 2022). This pilot program directly served five students, whose experiences we are currently in the process of evaluating. Their responses will help determine how well this model met our goals, and our findings will be published to help others with similar goals to build on our strengths and avoid the challenges we encountered.
- Constraining background and human-induced rates of mass export from the mountains to the ocean will demonstrate the impact of human land use on the Puerto Rican landscape. This research is important for the Puerto Rican community to know as they consider

agricultural and land use approaches, and more broadly can be compared to that of other regions to understand how different landscapes change and on what timescales. I will also contribute to the growing body of research on how large storm events affect our ability to accurately measure background erosion rates by comparing ^{10}Be concentrations collected before and after Hurricane Fiona, which occurred in fall 2022.

3. DISSERTATION CHAPTERS

3.1 Chapter 1: Reconstructing a record of landslides in Burlington, VT

Objective: to create a comprehensive record of historic landslides along Riverside Ave and explore patterns within available data to determine causality and management options.

3.1.1 *Background*

Landslides are a globally pervasive geologic hazard, occurring in all geologic settings and climate zones (Highland and Bobrowsky, 2008; Clague and Stead, 2012). Among natural hazards, at least 17% of global fatalities are attributed to landslides (Wallemacq, 2018). Globally, these hazards pose the greatest direct threat to human life and infrastructure when they occur in areas with high population and infrastructure density (Lacasse et al., 2009). Beyond direct damages, the indirect costs of landslides at the regional, community, and familial levels can be severe, long lasting, and difficult to estimate (Fleming and Taylor, 1980; MacLeod et al., 2005). Land use changes associated with urbanization, including forest clearing, slope steepening, the addition of unconsolidated fill material, and expanding infrastructure and impermeable surfaces, all increase the likelihood of landslide occurrence (Highland and Bobrowsky, 2008).

Landslides are caused by a combination of factors, including failure-prone geologic materials, steep topography, human-induced land-use change, and intense and/or long duration precipitation events that raise groundwater tables (Regmi et al., 2014). Instability can be exacerbated by leaking sewage and water lines (which increase pore pressure). In regions shaped by glaciation, such as Vermont, glacial sediment type and distribution can contribute significantly to landslide vulnerability (van Westen et al., 2003). Glacial outwash deposits, especially those dominated by sand, lack cohesion, and thus without root reinforcements, hold slopes no higher than the angle of repose (Perkins et al., 2017). Along river valleys, the already unstable nature of these materials is exacerbated by river incision, often along cut banks on the outer edge of meanders, which results in slope oversteepening and destabilization (Lévy et al., 2012).

Human actions play a significant role in determining landslide vulnerability. As we reshape landscapes for agriculture, urban expansion, natural resource extraction, and energy and transportation infrastructure, we destabilize natural systems, which can cause a cascade of effects. While landslides are naturally occurring geomorphic phenomena, the alteration of natural systems can exacerbate land instability, resulting in more frequent and larger landslides (Montgomery et al. 2000; Johnston et al. 2021). One common example is the addition of unconsolidated fill material onto slope surfaces to dispose of waste and/or to extend buildable area along the slope (Carey et al, 2021). Compounding forces such as deforestation, which removes root structures that stabilize slopes, and urbanization, which increases run-off from impermeable surfaces during storm events, also contribute to landslide probability (Cohen and Schwarz 2017; Johnston et al. 2021). For example, the deforestation of much of Vermont's old growth hardwood forests during the American colonial period caused the highest rates of hillslope erosion in the regional, post-glacial sedimentary record (Bierman et al. 1997). Here, I will use this historical context to answer my driving research questions: how many landslides have occurred along this road, what are the main drivers of these landslides, and are there spatial and/or seasonal patterns in landslide occurrence?

3.1.2 Methods

To evaluate the historical context and present landslide risk along an urban riverbank in Burlington, Vermont, I applied an interdisciplinary approach, examining the spatial distribution, timing, and cause of landslides affecting a 1.4 km stretch of road since 1952. After serving as a teaching assistant for geomorphology in 2020 where we investigated this case study, I compiled over 100 years of newspaper articles, maps, air and ground photographs, and written records along with boring logs and other zoning documents. I relied primarily on newspaper articles from the Burlington Free Press to build a record of historic landslides, and then compared these stories with maps and slope stability reports from the Department of Public Works records office. Using LiDAR imagery, I identified the landslide scarps and used spatial references from the historical materials available to determine the location and pattern of slope failure over time.

3.1.3 Results

I found that most mass movements along this corridor occurred on slopes over-steepened by the addition of unconsolidated artificial fill – added informally and without engineering considerations. These were mostly shallow translational landslides along with several deeper-seated rotational slides. While there have been no human fatalities, these landslides carried buildings, trees, garbage, junked cars, and segments of the roadway into the river below.

Through this investigation, I found that beginning in the 1920's, fill composed of junked cars, sand, gravel, concrete, and trash, was dumped over the edge of this 20-30 meter tall cut bank along the Winooski River. Over the following decades, at least 18 slope failures have occurred with a 3.9 year recurrence interval (range <1 – 11 years). Newspaper articles often attributed these slides to dumping and/or noted the presence of fill materials within the slide debris. While estimating landslide volume is difficult, newspaper records report that these landslides ranged in size from several to several thousand square meters of material (Figure 1). The majority of the landslides that had available date information occurred between August and October (2-3). I did not find record of any landslides occurring in December or January, and all other months had at least one landslide documented.

Today, those at risk from future slides along this road include small business owners, employees, homeowners, and tenants. The future looks increasingly unstable. Regional climate change predictions indicate a 10% increase in mean annual rainfall by 2100 over and above a nearly 20% increase since 1920 (Runkle, 2022). Paired with predicted increases in storm event frequency and intensity, future precipitation events will exacerbate slope hazards by raising ground water tables and thus pore pressure.

After reviewing potential management strategies and interventions, I recommend that the city incentivize the removal of structures built on fill and limit further filling activities through changes in zoning regulations and more effective enforcement of existing city codes. Interventions such as slope reinforcement, resloping, and restructuring and/or refurbishing existing drainage networks that may contribute to saturation-induced slope failures are costly and environmentally invasive. These methods have all been applied at least once along this slope within the past 80 years, with varying degrees of success. The most practical and low-cost response is for the city to purchase and remove existing infrastructure directly along the slope edge, and reforest the area to create a robust and stabilizing tree root network. The approach I use for analyzing this landslide hazard provides a framework for similar geographic settings and can inform urban planning and risk assessment within the context of climate change and pressures to develop marginal land as population increases.

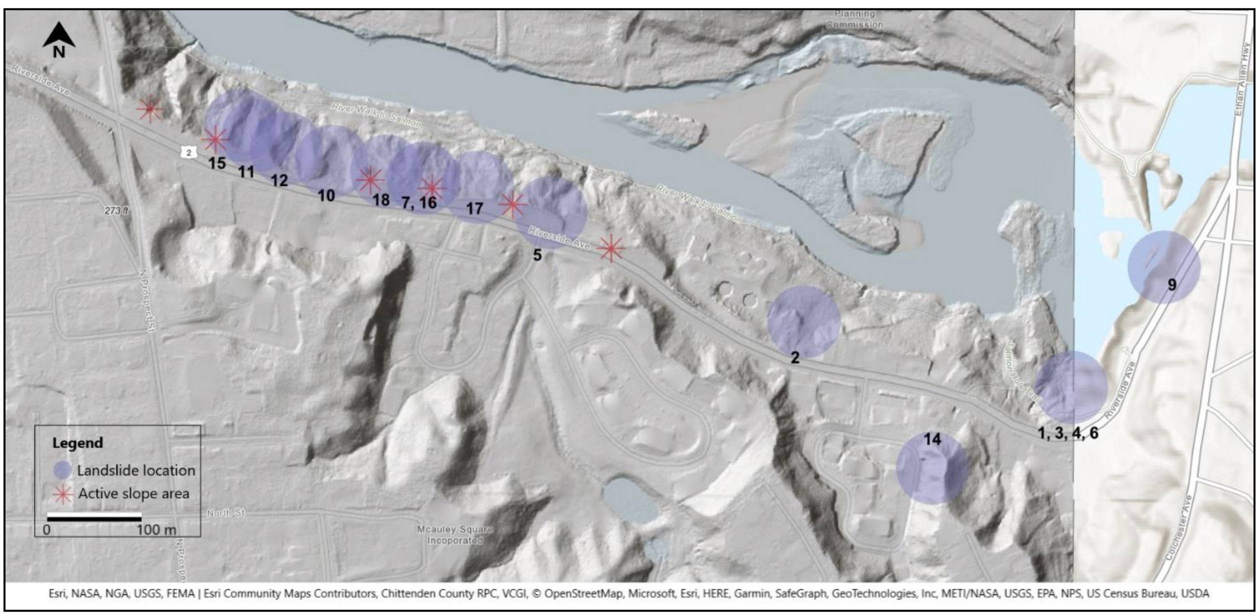

***Figure 1**: Map of landslide and active slope locations along Riverside Avenue, Burlington, VT. Purple circles denote areas of historic landslide activity and red stars mark areas of current slope instability. Each landslide is chronologically associated with a number (1-18) from earliest known slide to present, and these numbers correspond to rows in data table 1 (appendix).*

3.2 Chapter 2: Developing an undergraduate training program (AUGR)

Objective: to build a program model that successfully supports, prepares, and informs early career scientists from minoritized communities using best practice methods.

3.2.1 *Background*

The demographics of the North American environmental science community fail to represent the diversity of race, ethnicity, culture, and ability within the population (Huntoon & Lane, 2007; Levine et al., 2007; O'Connell & Holmes, 2011; Adetunji et al., 2012; Whittaker & Montgomery, 2012; Pearson & Schuldt, 2014; Callahan et al., 2017; Taylor, 2018; Bruthers & Matyas, 2020). This problem is compounded by the increasing societal demand for environmental scientists (Wolfe & Riggs, 2017) in growing fields such as data science, renewable energy, and geoscience (Sargent, 2014; *Fastest Growing Occupations*, 2022). Science training pathways are not yet meeting the recognized need for people with diverse perspectives and life experiences in designing approaches to address complex environmental problems, such as climate change and its impacts (Baber et al., 2010; Adetunji et al., 2012; Berhe et al., 2022).

To address this need, members of the environmental science community have sought to increase access and inclusion efforts in environmental science training opportunities. Such efforts have multiplied over the past several decades as more people have worked to identify, deploy, and evaluate effective strategies for recruiting and retaining members of underrepresented communities in STEM (Huntoon & Lane, 2007; Callahan et al., 2017; Wolfe & Riggs, 2017; Bruthers & Matyas, 2020). Programs to make environmental science research-training more available and equitable vary widely in size, scope, application, target age group, and demographics, as well as experiences offered and overall goals (Callahan et al., 2017; Wolfe & Riggs, 2017). These programs have varying levels of success (Roman & Logue, 2012; Follmer et al., 2017), underscoring the need for additional pedagogical development.

Recognizing both explicitly and implicitly biased elements of our current research training system, which often prioritizes students with more academically privileged backgrounds (Jack, 2019), I created an intensive, residential environmental science summer research training program (AUGR, Authentic Undergraduate Geoscience Research) designed to include students based on their motivation to learn rather than their academic record. AUGR delivers many of the benefits of the National Science Foundation (NSF) Research Experiences for Undergraduates (REU) model, but is open to students who may not yet have the academic credentials and experiences needed to obtain admission to an REU. I designed the AUGR model using established strategies for student engagement and retention in earth sciences (Huntoon & Lane, 2007; Wolfe & Riggs, 2017, Knight, 2022) to build a program specifically aimed at engaging students from groups underrepresented in environmental science (Figure 2). My goal was to actively dismantle the obstacles that may otherwise stand in the way of participants' continuation and successes in STEM and provide them with the support necessary to overcome obstacles in their future endeavors. This project responds to the need for establishing well-documented, effective program models that can be used by the broader research community (Wolfe & Riggs, 2017).

3.2.2 *Methods*

I designed AUGR as an experience that would support, challenge, and encourage students as they engaged in learning experiences designed to facilitate personal and professional growth. I began with the goal of creating a learning environment in which students could develop confidence and a sense of belonging in STEM, which is integral to developing a scientific identity (Dutt, 2020; Bernard, 2020). As a structure for creating this environment, I chose the undergraduate research experience model, and integrated six supportive structures: mentoring, training in new skills, network expansion, an intentional cohort community, and non-extractive place-based research within a financially and academically accessible model. With this structure, I aimed to make the student experience fun and accessible, in turn increasing the likelihood of student success in achieving growth in both the personal and professional spheres.

Professionally, I immersed participants in key aspects of environmental science, including collaboration with team members, fieldwork, laboratory work, data analysis, and public presentation (Figure 2). Throughout these stages of the program, I trained students in specific skill sets that are critical for the development of a technically literate STEM workforce (Figure 3). On a personal basis, I wanted the students to have a positive experience as part of a living and learning community, make new friends and connections, and explore their interests with new perspectives and approaches.

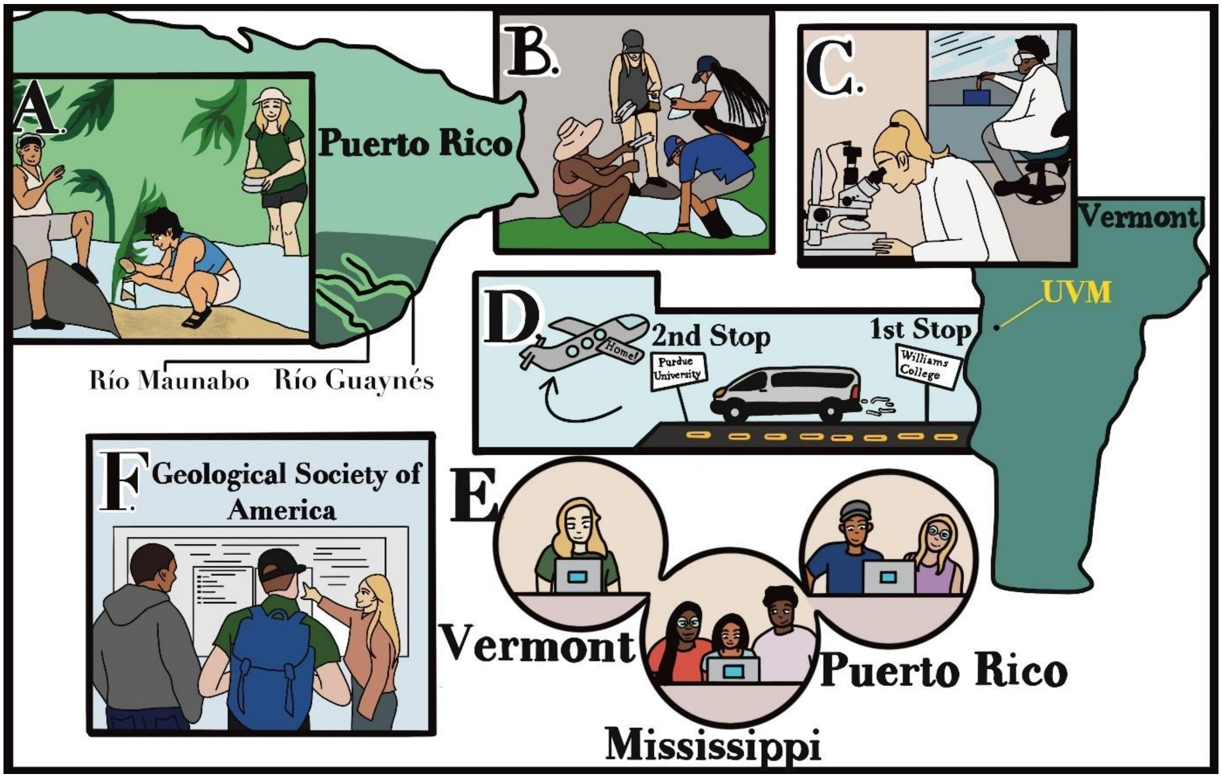

Figure 2*: Artistic representation of the AUGR program stages. (A) program preparation and field reconnaissance; program leaders learning about local land use change from a community collaborator. (B) field research training; students working together to collect field samples and measurements at a field site. (C) laboratory work and interdisciplinary exploration; one student working in the NSF/UVM Community Cosmogenic Facility (right) and another student using a microscope as part of our interdisciplinary training series (left). (D) visits to other laboratories; the order of events during the final segment of the summer experience. (E) remote conference preparation; participant locations. (F) conference attendance and presentations; a participant presenting their poster to an audience of two. Illustration by Shay Taylor.*

I designed the student research project to engage students in real and relevant scientific investigation and factored both physical accessibility and time considerations into the project design. For field work, I selected two adjacent watersheds in southeastern Puerto Rico to compare using a variety of environmental indicators, with the goal of providing students with a novel and interdisciplinary curriculum and research training platform. One of the limiting factors in field site selection was the necessity of sampling quartz-bearing basins for cosmogenic beryllium-10 (^{10}Be) analysis, which the students would participate in during their time at UVM to measure rates of erosion (Bierman & Steig, 1996; Granger et al., 1996). Using a combination of GIS, Google Maps, and field reconnaissance with the help of Krizzia Soto-Villanueva, I selected a total of 19 study sites, distributed evenly between the two watersheds. These sites span from the highest tributaries to the lowest point along the main branch before each river enters cultivated farmlands. To provide participants with context for what insight they would gain from this project, we established four guiding questions (Figure 3, lower left).

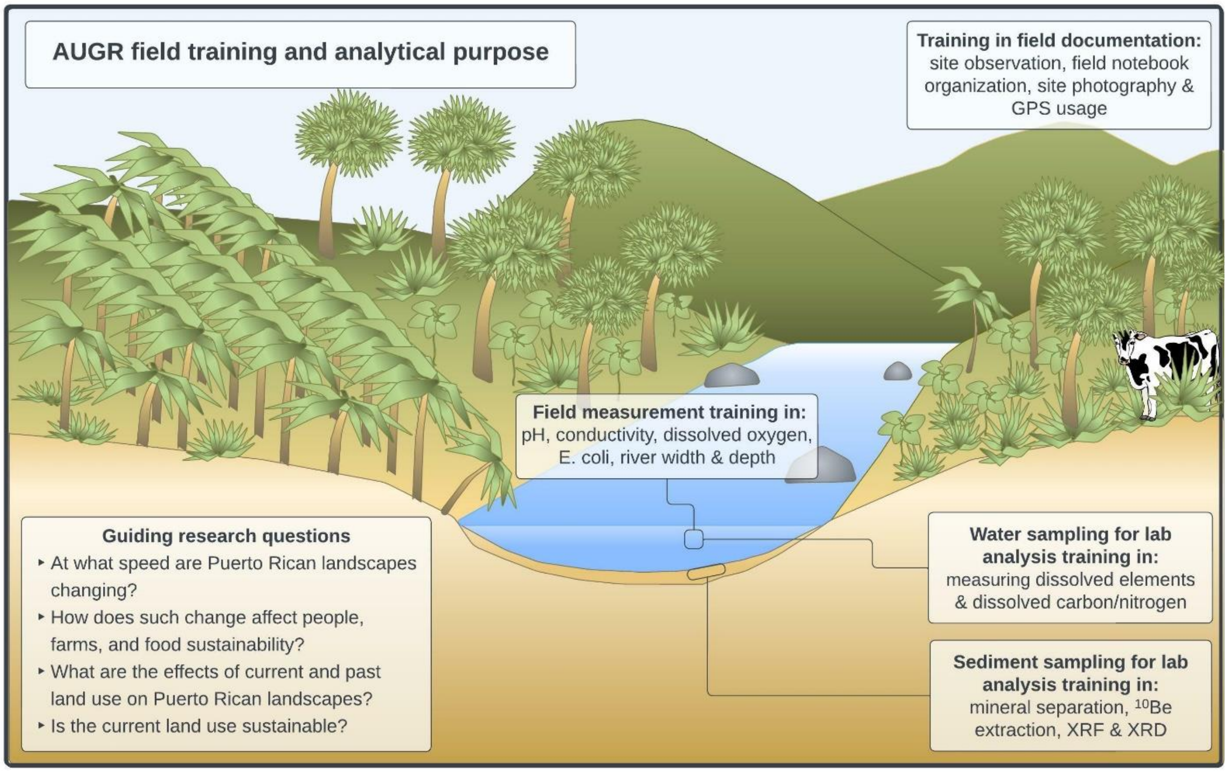

Figure 3: *Visualization of the overarching scientific goals of the program, as well as the measurements collected at each field site and subsequent analyses. The landscape shown represents a typical field site, and callout boxes indicate where each type of sample was collected. The foreground of this figure represents sites at lower elevations, which were proximal to farm lands with cultivated banana and plantain trees (shown on left) or used for cattle ranching (right). The background represents the mixed forestation of the mid to higher elevation sites, which were characterized by dense, diverse, and uncultivated vegitation.*

3.2.3 Preliminary results

Through AUGR, I learned that the most effective approach for educating motivated undergraduate students who lack prior research experience is to scaffold each learning module from a foundational level through the required level of competency. Based on my observations (and those of my mentors and project co-leadership) this program had several key successes and several weak points that I hope to have the opportunity to improve on in the future.

Some of the successful components of program design included recruiting a strong pool of applicants across a wide range of STEM disciplines, selecting five individuals who together formed a supportive and respectful cohort, creating an exciting, hands-on series of experiences for the students, and introducing them to more than two dozen scientists along the way. Training wise, students successfully mastered all of the field sampling techniques, participated thoughtfully and intentionally in lab work in several different lab settings, and reported being excited about all of these experiences both formally (Howard, 2022) and informally. During their time at UVM, the students reported interest in attending graduate school after finishing their undergraduate degrees, which may link to increasing feelings of inclusion and sense of belonging in the STEM community. Four out of five students completed posters for public presentations (despite a water crisis in Jackson, MI, and the aftermath of Hurricane Fiona in Puerto Rico). Upcoming student interviews will evaluate the student's perceptions of the program and help us to formally evaluate which aspects they found successful and which should be rethought.

During and after this program, I identified several areas of design weakness. Overall, weakness stemmed from condensed timelines and unrealistic expectations of participants' prior training, which lead to insufficient scaffolding. This was most evident during the abstract writing and poster creation processes, which required student data analysis and interpretation that the students were not adequately nor evenly prepared to do. This resulted in varying levels of confusion and overwhelm for both the students and me, and one student left the program. To address this issue, I would change two key aspects of the program. First, I would begin the recruiting and application process earlier in the year to make time to teach foundational concepts prior to the in-person program. Second, I would expand emphasis on building analytical and science communication skills in-person, and restructure the conference preparation portion of the program to occur during the in-person segment, limiting virtual instruction. These revelations, soon to be paired with student interview data and published, will provide a starting point for similar programs to build from and improve upon. By sharing this approach, I hope to contribute to the ongoing work of intentionally expanding STEM inclusivity and accessibility.

3.2.4 Ongoing work

I am currently coordinating participant interviews to take place in June/July 2023 (timing depends on IRB approval). I have prepared a list of interview questions, and my colleague, Veronica Sosa Gonzalez, will perform one-on-one interviews virtually. Veronica met the students in June 2022, but is otherwise a neutral party for participants to share their reflections with. The purpose of these interviews is to gather student perspectives on the program stages and outcomes to assess whether my observations, summarized above, align with those of the students. This input is crucial for evaluating the effectiveness of the AUGR model in meeting its foundational goals.

3.3 Chapter 3: Quantifying mass export in Puerto Rico

Objective: to understand the flux of material – sediment and dissolved load – from the Puerto Rican landscape into the ocean, in the context of natural and human forcings.

Terminology

There are several key terms and concepts I will refer to regularly throughout this chapter. For clarity and continuity, I have defined and provided a bit of context for each below.

Term	***Definition***
Basin	While drainage basin and watershed are often used interchangeably, I will use the term basin to describe a watershed subunit in the context of this project. Each field site described in this chapter is located within one of two watersheds and sits at the bottom of a topographically defined catchment. I will refer to these catchments as basins.
In situ Cosmogenic ^{10}Be	Cosmogenic beryllium-10 is a radioactive isotope that forms when high energy particles from space (cosmogenic) interact with silica or oxygen atoms in minerals and cause the ejection of protons and neutrons from the atom's nucleus. These reactions occur close to the earth's surface, primarily in the upper three meters of rock. ^{10}Be accumulates in minerals at known rates and can be used to estimate background (naturally occurring) rates of erosion (Dunai, 2010; Lal, 1967, 1991). Here, I estimate erosion rates using the concentration of ^{10}Be formed within the mineral quartz (*in situ)*, which I extracted from stream sediment.
Denudation	Denudation refers to the combined processes by which mass is exported off of a landscape. As a concept, it describes the weathering of rock into both sediment and dissolved ionic compounds, as well as the processes that transport these materials. Denudation is measured as the sum of the material lost, and therefore includes both solute and sediment fluxes.
Erosion	Erosion refers to the mechanical weathering processes that generate and transport sediment. In this chapter, I quantify erosion using cosmogenic ^{10}Be.
Short-lived isotopes	Several radioactive isotopes with short (days to years) half-lives can be used to deduce information about erosion on human timescales. For this project, I will use a gamma-ray detector to detect ^{137}Cs and ^{210}Pb in stream sediment. ^{137}Cs was formed and distributed through atmospheric nuclear weapons testing, which began in 1952 and peaked in 1963 (Singleton et al, 2016; Du et al, 2011). ^{210}Pb forms in the atmosphere as the decay product of ^{222}Rn, and is primarily transported via precipitation to the earth's surface (Singleton et al, 2016; Du et al, 2011). ^{7}Be forms similarly to ^{210}Pb, and both are heavily influenced by precipitation, latitude, and seasonality (Du et al, 2011).
Watershed	A watershed is an area of land that drains to a common outlet. Watersheds are separated from each other by drainage divides, or local maxima. I collected field samples for this project in two adjacent watersheds, each of which is drained to the ocean by a river originating in the mountains. Each watershed in this study is referred to by the name of its respective river, Río Maunabo or Río Guayanés. Field sites in the Río Maunabo watershed begin with PRM while sites in the Río Guayanés watershed begin with PRS.

Background

The landscape of Puerto Rico is dominated by the Cordillera Central, an east-west trending mountain range (up to 1,338 m in altitude) that makes up 75% of the island's area (Bienroth, 1969). These mountains are primarily interbedded marine volcanic and sedimentary rock that formed during the cretaceous through Eocene (145-35 Mya) (USGS, n.d.). Tectonic activity, caused by the convergence of the Caribbean and North American plates, has extensively folded and faulted these layers (Cheadle, 2015). During the late Cretaceous, several igneous plutons of granodiorite to diorite composition intruded and crystallized under the island (Monroe, 1980; USGS n.d.). Within the last 30 million years, limestones formed along the northern and southern flanks of the island (USGS, n.d.). From the Cordillera Central, short, incised rivers travel down gradient, across coastal plains, and into the ocean (Bienroth, 1969; USGS, n.d.). Over time, these erosional processes have formed alluvium deposits around the perimeter of Puerto Rico, and to a much lesser extent within the interior (USGS, n.d.).

A 500-year long history of colonialism has shaped the political, social, agricultural, economic, industrial, and thus land-use systems of Puerto Rico (Caban, 2005). Puerto Rico is the smallest of the Greater Antilles Islands (8,858 km^2) and is presently home to more than three million people (U.S. Census Bureau, n.d.; Beinroth, 1969). When the Spanish initially colonized Puerto Rico in 1508, there were 30,000 indigenous Taíno people living in communities across the island (Fisk, 2022; Schimmer, n.d.). Pre-colonization, the Taíno people used the landscape to construct villages, forage for food, and cultivate crops including yuca, sweet potato, and corn (Fisk, 2022). In the first 20 years of Spanish rule, the Taíno people were subjected to enslavement and disease to the extent that less than 1200 Taíno people were recorded in the 1530 census (Schimmer, n.d.). The Spanish then imported African slaves to maximize gold mining and agricultural production. As the gold reserves quickly diminished, the focus shifted to cash crops, with increasingly widespread cultivation of tubers, grains, tobacco, vegetables, and fruit, which persisted through the end of slavery in Puerto Rico in 1873 (Schimmer, n.d.). In 1898, the United States took control of Puerto Rico and by 1910, the agricultural census reported that more than 92% of the island was cultivated (Figure 4) (USDA, 1964). At this time, coffee was cultivated in the mountainous central region, sugar and grass grew along the flatter coastal perimeter, and bananas, oranges, and tobacco farming filled the landscape between (Figure 4). Since then, the percentage of land used for agriculture in Puerto Rico has been in decline, dropping to 72% by 1964, and to 21% by the most recent census in 2017 (USDA, 2017, 1987, 1964).

The United States government has made all major decisions regarding Puerto Rican land use and agriculture since it became an unincorporated territory in 1898 (Caban, 2005). Following World War II, the United States shifted Puerto Rico's agricultural focus to industry, and later to pharmaceutical production (Caban, 2005; Galarza, 2015). This history of colonial, export-driven economic decisions has had significant impacts on the Puerto Rican people and landscape. Today, Puerto Rico is more than 85% reliant on imported food, a major shift over the course of a century (Marrero et al, 2021). Puerto Rico's history informs the data we acquire today and how we interpret it, as historic land use and disturbance impart measurable geochemical signals.

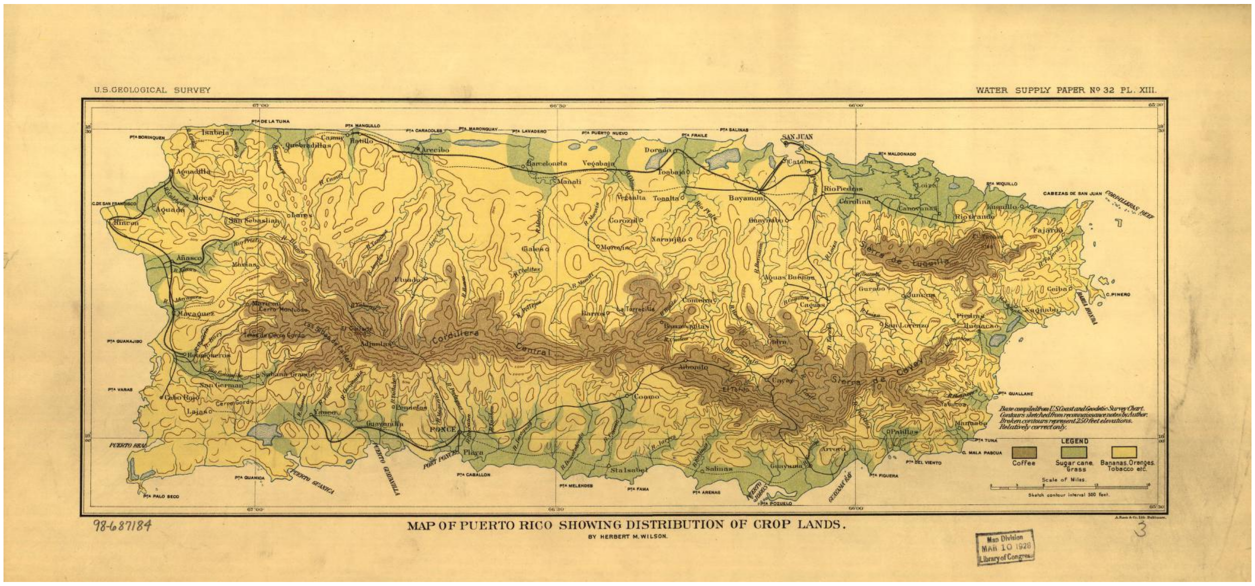

Figure 4: *1898 map of crop distribution in Puerto Rico. A US Coast and Geodetic Survey map showing crop distribution using three crop groups by color. Brown represents coffee, green represents sugarcane and grass, and yellow represents bananas, oranges, tobacco, and other unlisted crops.*

For this project, I will measure rates of mass loss from the landscape to evaluate the impacts of human-landscape interaction in Puerto Rico at the watershed scale. Mass loss is driven by weathering, which liberates material, and hydrologic processes, which transport material. In the tropics, climate and precipitation drive physical and chemical weathering, while biological processes drive mechanical weathering (Earle, 2015). Southeastern Puerto Rico's warm, wet environment induces rock weathering through a combination of chemical dissolution and the formation of secondary minerals such as clays (Perdrial et al., 2015). These products of weathering – dissolved solute, secondary minerals, soil, and mobilized sediment – are susceptible to erosion and transport by precipitation, groundwater, and overland flow, leading to their eventual deposition within a stream, and later into the ocean (Stallard, 1988). While the tropics occupy less than a quarter of the earth's landmass, they contribute disproportionately high sediment (~50%) and dissolved solute fluxes (38% of total ionic load) into the ocean by way of river transport (Stallard, 1988). In this way, tropical streams are crucial to global solute and sediment cycling.

At the basin scale, sediment geochemical composition and stream water isotopic composition reflect the geology of the upstream area. This is an important concept in geomorphology, as we use several different geochemical and isotopic approaches to quantify mass loss over various timescales and pathways within watersheds. We measure background (long term, naturally occurring) erosion rates using *in situ* produced cosmogenic ^{10}Be, which has a half-life of ~1.4 My (Dunai, 2010; Lal, 1967, 1991). To exploe erosion on human timescales, we use ^{7}Be, ^{210}Pb, ^{137}Cs, which have half-lives ranging from days to decades (Singleton et al, 2017). These isotopes are generated either within a rock (*in situ)* through atomic level nuclear reactions (^{10}Be) or in the atmosphere and transported into stream networks via precipitation (^{7}Be, ^{210}Pb, ^{137}Cs) (Singleton et al., 2017). We quantify mass loss via dissolution by measuring the major cations and anions within river water samples and then extrapolate annual flux based on annual discharge measurements, in this case from USGS gauging stations (USGS, 2023a, b).

Throughout the tropics, these methods are increasingly applied together to quantify mass loss more accurately and constrain the effects of land use and storm events on the landscape (Bierman et al., 2020; Grande et al., 2021; Quock et al., 2021; Campbell et al., 2022). Previous studies in Puerto Rico have investigated weathering and dissolution in the Luquillo region (White et al., 1998; Kurtz et al., 2011; Lara et al., 2017; Moore et al., 2019). Other studies have determined rates of surficial erosion using *in situ* cosmogenic ^{10}Be (Brown et al., 1995, 1998; Riebe et al., 2003; Riebe & Granger 2013; Brocard et al., 2015).

Two recent studies provide the foundation for the project described in this chapter. Campbell et al. (2022) investigated the relationship between erosion (measured using cosmogenic ^{10}Be and ^{26}Al) and rock dissolution in Cuba, using many of the same or comparable methods as those described below. This study demonstrates the significance of mass loss through dissolution in humid, tropical regions. To estimate total mass loss (denudation), Campbell et al., (2022) suggest that in areas where dissolution measurements exceed ^{10}Be-derived erosion rates, dissolution measurements can provide a lower limit of denudation. To establish an upper limit of denudation, Campbell et al. (2022) the sum of measured dissolution and ^{10}Be-derived erosion rates for each watershed.

To quantify the effects of large storms on measurements of erosion using ^{10}Be, Grande et al. (2021) sampled *in situ* and meteoric ^{10}Be in Luquillo, Puerto Rico repeatedly over 18 months following Hurricane María. This study was situated in two nested watersheds where the hurricane triggered landslide activity. Grande et al. (2021) show that ^{10}Be concentrations in stream sediment do not change uniformly following a storm event. While the concentration in one stream did not change, the concentration in the other increased linearly for the duration of the study, rebounding from an influx of low-concentration sediment due to landslide activity. This study demonstrates that samples collected within 1-2 years after a large storm event may result in over-estimations of background erosion rates (Grande et al, 2021).

As in Grande et al. (2021), previous cosmogenic ^{10}Be erosion research in Puerto Rico has primarily been conducted in the northeastern part of the Island, which is situated within a granitic lithology, providing ample quartz for analysis (Brown et al., 1995; Brocard et al., 2015; Grande et al., 2021). My field area, in southeastern Puerto Rico, has a similarly quartz-rich granitic lithology, yet lacks previous background erosion rate measurement using ^{10}Be, providing an opportunity for regional comparison and a broader understanding of mass loss across Puerto Rico (Figure 5). With this study, I intend to 1) constrain denudation rates within the study area using the parameters set out by Campbell et al. (2021), 2) investigate whether Hurricane Fiona

(September, 2022) had a measurable effect on *in situ* ^{10}Be in my field area, 3) explore the geochemical differences in the two watersheds that form my study area, and whether these differences have an affect on rates of mass loss.

Field Area

The research discussed in this chapter is situated in two adjacent watersheds in southeastern Puerto Rico. This region is tropical and receives an average of 183 cm of precipitation per year (NWS, n.d.). The bedrock geology in this area is primarily cretaceous granodiorite to quartz diorite, however there is some volcanic material within the higher elevation basins, and alluvium in the lower elevation basins (Figure 5) (Bawiec, 1998). My field sites are distributed along the tributaries and main branch of each basin's major river. Sites range in altitude from 302 m to 13 m. The basins drained by each field site vary in size from 0.05 km^2 (the smallest nested basin) to 9.8 km^2, though some also drain into one another, enlarging their upstream catchment areas.

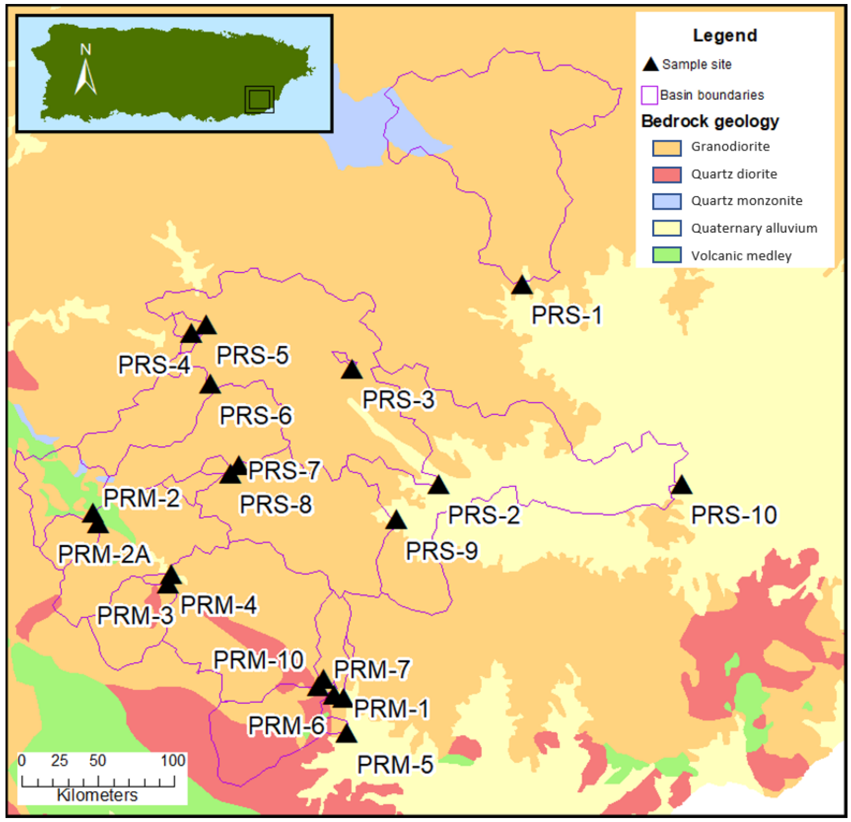

Figure 5: *Simplified lithology within and proximal to sample basins. This section of Puerto Rico is dominated by cretaceous granodiorite, with some similarly aged quartz diorite and quartz monzonite formations interspersed. Quaternary alluvium includes several small landslide deposits (not shown). Volcanic medley refers to a metavolcanic formation (Bawiec, 1998; Krushensky, 2000). Sample site names beginning with PRM are within the Río Maunabo watershed, while site names beginning with PRS are within the Río Guayanés watershed.*

3.3.1 Methods

I use stream water and sediment collected at each field site to quantify the materials exported by these two stream networks. Using stream water, I measure and sum major dissolved cations and anions to quantify mass loss through rock dissolution. I will use a combination of short-lived and long-lived radiogenic isotopes from stream sediment samples to measure how human land use has affected erosion rates in Puerto Rico. First, I will use *in situ* cosmogenic ^{10}Be to establish background (geologic time-scale) rates of erosion. Then, to ascertain how human land use has accelerated erosion in Puerto Rico, I will measure short-lived isotopes ^{137}Cs (half-life =30.2 years), and ^{210}Pb (half-life = 22.3 years) (Singleton et al., 2016).

Field Site Selection

I selected field sites to create a representative sample of two watersheds and their respective major tributaries. I used aerial imagery to identify 50 potential sites, and then traveled to Puerto Rico to assess them. Each site I selected for sampling met three requirements: 1) it contained quartz-bearing river sediment, 2) the sampling location was physically accessible, 3) the site was located on public land, or the landowner granted us access. I found 19 sites that met these criteria: nine in the Río Maunabo watershed, and ten in the Río Guayanés watershed (Figure 5).

Field Methods

At each field site, Krizzia Soto-Villanueva and I (and the AUGR participants in June 2022) collected stream water and sediment samples. The sediment samples were collected for ^{10}Be extraction, XRF, and short-lived radionuclide detection. To ensure we had the right amount and size fraction of sediment for each type of analysis, we collected two bags of sediment at each site: one bag of 250-850 µm grains and one bag of finer-grained sediment. To collect the 250-850 µm sediment, we sieved sediment from within the stream channel to this grain size. To collect the fine-grained sediment, we searched for a depositional feature - such as a point bar or sandbar - and collected the fine material there.

We also collected both filtered and unfiltered water samples at each site. To collect unfiltered water, we precontaminated a 125 mL sample bottle by filling and emptying it two times in the stream before filling and capping it. To filter water samples, we used a sterile disposable 20 mL syringe and a screw-on 0.45 µm nylon filter tip. We collected a 15 mL centrifuge tube of filtered water at each sample site. These samples were collected from the center of the river at each site, and below the surface.

We measured E. coli at each sample site using Aquagenx CBT EC + TC kits. We prepared each kit at the respective field site following the instructions for use (Aquagenx, n.d.). We used a a 1:10 dilution ratio of river water to store-bought drinking water. We then kept the kit in a warm, dark area for at least 24 hours before reading the results using the provided E. coli Most Probable Number Table. Afterwards, we decontaminated each test kit using bleach.

We collected field measurements at each site, including GPS coordinates, elevation, water temperature, pH, dissolved oxygen (DO), conductivity, and representative stream width and depth. We used respective meters to measure temperature, DO, and conductivity, and pH papers to measure pH. We also recorded field observations in a field notebook and took photos at each field site to record site characteristics and any features of note.

<u>*Laboratory Methods*</u>

I collected sediment and water samples for several purposes, and describe each method of preparation and/or instrumentational analysis below. Directly after field collection, I kept water samples refrigerated or on ice to preserve the chemical composition. Once back in Vermont, I dried sediment samples in a 60° oven.

Water sample analyses

Each of the following water sample analyses were completed on all field samples from both March and June. This work was completed as a joint effort between the AUGR students, the respective laboratory PIs, their students, and I. At Williams College, where we did the majority of our water geochemistry, we used a Perkin-Elmer Atomic Absorption Spectrometer to measure major cations (Ca^{2+}, Mg^{2+}, Na^{2+}, K^{+}, Nh^{4+}), and a Metrohm 883/863 Ion Chromatograph to measure major anions (HCO_3^-, Fl^-, Cl^-, NO_3^-, HPO_4^-, NO_2^-, Br^-) in our water samples. We measured silica using a Technicon Autoanalyzer II, and bicarbonate using a Radiometer Analytical AutoTitrator. We also used a FisherSci pH meter to measure pH, and a Hach Field conductivity meter to measure conductivity of unfiltered water. At UVM, we measured dissolved organic carbon (DOC) and total dissolved nitrogen (TDN) in filtered water samples using a Shimadzu TOC-L Analyzer. We also used an ICP-OES at UVM to measure Ca, Fe, K, Mg, Na in filtered water samples, to compare with and augment major cation geochemistry data collected at Williams.

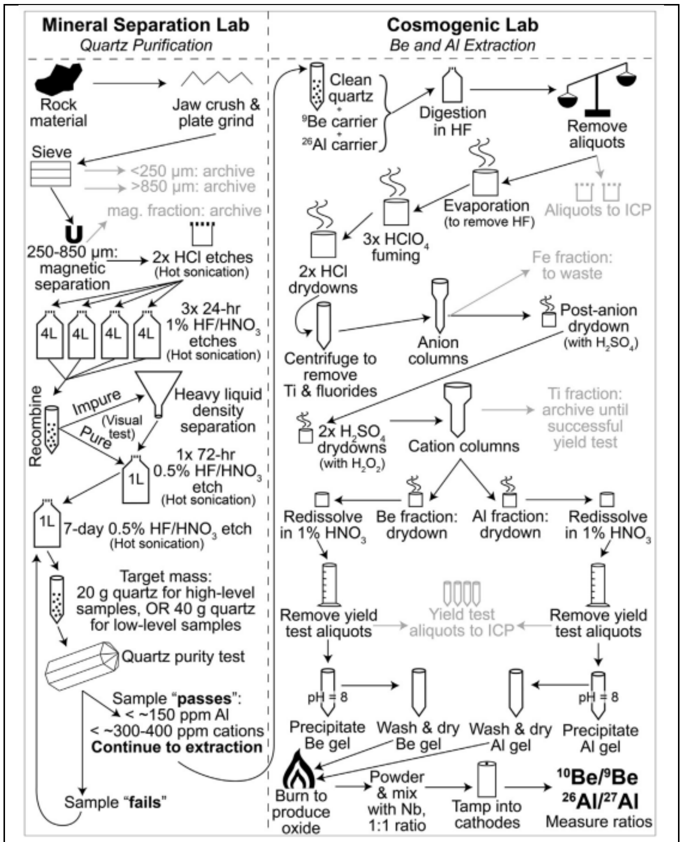

Figure 6: Illustrated and optimized sample preparation process for cosmogenic ^{10}Be extraction from quartz grains. (Corbett, et al. 2016)

Sediment sample analyses

^{10}Be extraction: After field work, I prepared the 250-850 μm sediment fraction for beryllium extraction (Figure 6, left side) (Kohl and Nishiizumi, 1992; Corbett et al, 2016). Using the ^{10}Be extraction procedure (Figure 6, right side) I extracted ^{10}Be from my samples. After the first extraction, the AUGR students and I traveled to the Accelerator Mass Spectrometer at Purdue PRIME laboratory to count the atoms of beryllium and convert these values to erosion rates.

Short-lived isotopic analysis: Samples are currently being analyzed for ^{210}Pb and ^{137}Cs gamma radiation using germanium detectors at Oberlin College. During fall 2022, I sieved the bulk sediment sample from each basin to isolate the fine material (<63 μm). I then prepared a fine-grained vial for every field site, and a coarse-grained sample (250-850 μm) for 12 of the sites. For the fine-grained samples, I measured and recorded a mass of between 1.5-30 g of material into 20mL vials. For the coarse-grained samples, I measured 200-300 g of each sample into a 4 oz container, recorded the sample mass, and sealed the lid. I also measured and recorded the sample thickness for every sample, in order to estimate sample volumes. I then mailed these samples to Oberlin College, where they remained sealed for at least 21 days before being individually analyzed in a gamma radiation detector. Each sample was or will be measured for 24 hours, and samples with high uncertainty will be measured again for 96 hours. *We are not measuring* ^{7}*Be because too much time, and thus radioactive decay, elapsed between sample collection and detection, however I hope to measure it following my next field season.*

X-Ray Fluorescence (XRF): I prepared each sample for XRF analysis by fluxing using a Claisse LeNeo Fluxer at Middlebury College. First, I powdered 5 ml of the 250-850 μm fraction of each sample using a ball mill. Next, I dried each sample thoroughly in a porcelain crucible using a muffle furnace at 1000 degrees C for 15 minutes. After these samples cooled in a desiccator, I used the Claisse LeNeo fluxer to combine 0.8 g of dried sample material with 8.0 g of flux material (lithium tetraborate) into a glass disk for XRF analysis. Once the disks were created, I used a Thermo Fischer ARL Quant'X XRF to measure the elemental composition by percentage in each sample. *I have completed half of this analysis and will prepare and analyze the remining samples over the summer.*

Calculations

Dissolved load: I estimated the mass moved from the land to the ocean as dissolved load for each watershed. First, I downloaded mean annual flow data from the USGS river gauging station in each of the study area watersheds (USGS, 2023a,b) and averaged mean annual flow in m^3/yr for the period of record (Maunabo, 44 years; Guayanes, 20 years). Next, I converted all cation and anion measurements from mg/L to mg/m^3, and multiplied these by the mean annual flow, resulting in ion flux in mg/yr. Then to normalize flux over basin area, I divided ion concentration (mg/yr) by basin area (km^2), and converted from km^2 to m^2, producing mass flux values for each cation and anion in g m^{-2} yr^{-1}. I estimated annual dissolved flux by summing the annual flux of all major cations and anions.

^{10}*Be erosion rate:* Once I received the measured ^{9}Be/^{10}Be ratios from the Purdue PRIME laboratory, I calculated the number of atoms of ^{10}Be per gram of quartz for each field site, as well as the uncertainty, using the blanks from each sample batch. Then, I used "The online calculators formerly known as the CRONUS-Earth online calculators" (Balco, 2017) to calculate an erosion rate for the basin area upstream of the sample site.

Establishing upper and lower bounds on mass loss: Following the model in Campbell et al. (2022), I summed the average annual watershed dissolved load and ^{10}Be erosion rates to establish a maximum total denudation value for each watershed. Given that ^{10}Be derived erosion rates only represent the top three meters of material and tropical soils often weather to much greater depths, I will use the dissolved solute load to estimate minimum denudation values. This decision is in agreement with the approach used in Campbell et al. (2022).

Geographic Information Systems (GIS):

I will use GIS to calculate geologic, land use, and land use change spatial statistics. I will also use GIS to calculate the appropriate cosmogenic ^{10}Be production rate of each watershed based on the mean latitude, mean longitude, and altitude, a concept described as effective elevation (Portenga & Bierman, 2011). I will then investigate the spatial relationships within and between these variables and the full data set.

3.3.3. Preliminary results

Now that much of the data for this project has been collected, I am in the beginning phase of data analysis. I plan to spend much of my remaining time at UVM focusing on analyzing and interpreting these data. Here, I will share some of my initial data exploration and findings.

^{10}Be derived erosion rates & dissolved solute flux

I found that there is some variation in quantity of eroded material between the adjacent Río Maunabo and Río Guayanés watersheds (Figure 7). The Río Maunabo watershed is eroding at an average rate of 174 g m^{-2} yr^{-1}, while the Río Guayanés watershed is eroding at an average

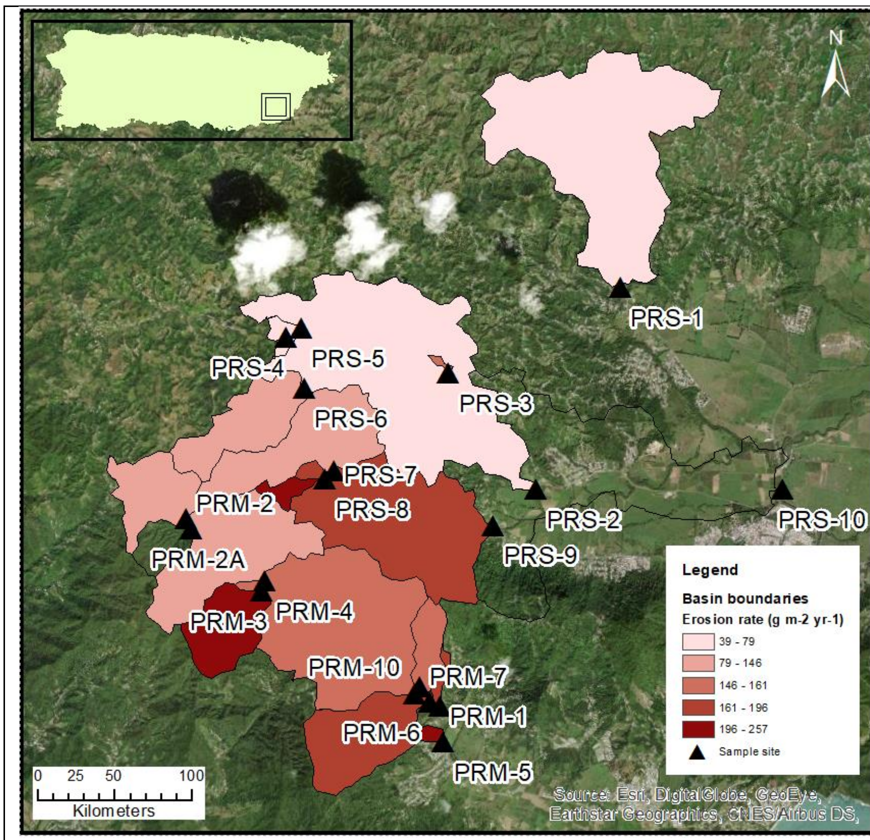

***Figure 7:** Map of basin erosion rate values by color. Basins with low erosion rates are shown in light pink, while those with high erosion rates are shown in dark red. Note: PRM-2A and PRS-10 have not yet been measured, so these watersheds are delineated but not filled. Base map sources: ESRI, DigitalGlobe, GeoEye, Earthstar Geographics, CNES/Airbus DS.*

rate of 110 g m^{-2} yr^{-1} (Figure 7, 8). Across both watersheds, the average rate of erosion is 138 g m^{-2} yr^{-1}. The equivalent erosion rate (normalized by density) in meters per million years (m/Myr) for Río Maunabo is 67 m/Myr (range: 49 – 90 m/Myr; standard deviation 14), and 42 m/Myr (range: 15 – 99 m/Myr; standard deviation: 27) for Río Guayanés.

Dissolved solute loads for each watershed are similar to or higher than average ^{10}Be erosion rates (Figure 8). The calculated annual dissolved solute load for Río Muanabo was 216 g m^{-2} yr^{-1}, while Río Guayanés was 112 g m^{-2} yr^{-1}. While the dissolved solute flux and erosion rate in Río Guayanés were similar (110 vs. 112 g m^{-2} yr^{-1}), the dissolved solute flux in Río Maunabo was greater than the erosion rate by > 40 g m^{-2} yr^{-1} (Figure 8).

Together, these datasets establish upper and lower bounds on denudation for each watershed. The maximum denudation rates, (the sum of erosion and dissolved solute flux) are 390 g m^{-2} yr^{-1} (Río Maunabo) and 222 g m^{-2} yr^{-1} (Río Guayanés). Using dissolved solute measurements as the minimum boundary on denudation for each watershed, total denudation in Río Maunabo is between 216 and 390 g m^{-2} yr^{-1}, and between 112 and 222 g m^{-2} yr^{-1} in Río Guayanés.

For context, Campbell et al. (2022) estimated dissolution rates between 10 – 126 g m^{-2} yr^{-1}, and ^{10}Be derived erosion rates between ~3 – 189 g m^{-2} yr^{-1} (maximum rate: 16 – 298 g m^{-2} yr^{-1}) across 26 watersheds in central Cuba. These data from Campbell et al. (2022) represent a far more varied lithological setting than the two watersheds within my study, and demonstrate the relationship between lithology and the ratio of dissolved solute to erosion flux. If we compare results between these studies, the upper and lower limits of denudation for Río Guayanés are within the range Campbell et al. (2022) measured in Cuba, though the solute flux is high by comparison. In the Río Maunabo watershed, the measured upper and lower bounds on denudation are both 2.6 standard deviations above the average upper limit measured by Campbell et al. (2022).

***Figure 8:** Measured erosion rates grouped by watershed & compared with solute export values. The erosion rate plots demonstrate the range of erosion rates within each watershed, and can be compared to the calculated solute flux values. The "X" symbol within each box plot represents the mean, while the whiskers represent the range of data included.*

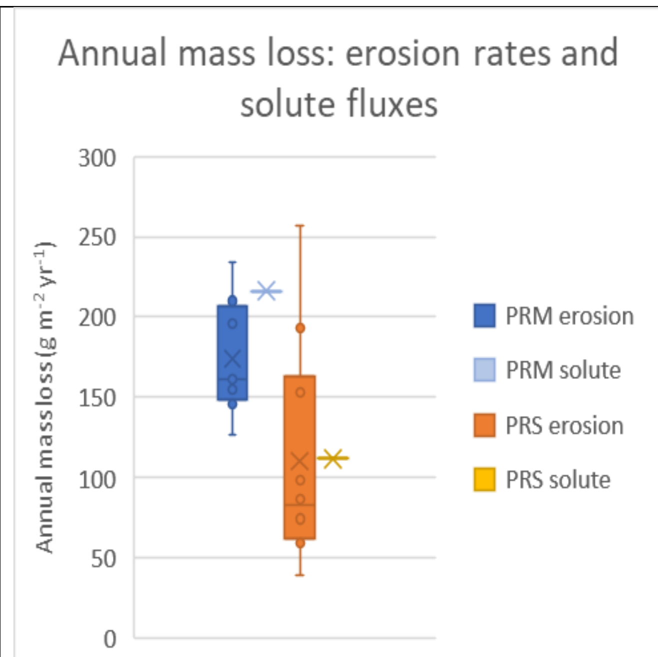

Within the total solute flux, several key compounds make up the majority of dissolved material in both watersheds, including bicarbonate (HCO_3^-), calcium (Ca^{2+}), chloride (Cl^-), and sodium (Na^+) (Figure 9). Bicarbonate accounts for 56% of the total mass flux in Río Maunabo (121 g m^{-2} yr^{-1}), and 53% in Río Guayanés (59 g m^{-2} yr^{-1}). In Río Maunabo, other major contributors to total dissolved solute include Ca^{2+} and Na^+ (11% each), and Cl^- (8%). In Río Guayanés, other major contributors include Na^+ (12%), and Cl^-, Ca^{2+}, and SiO_2 (9% each). The Na^+ and Cl^- values shown in Figure 9 are likely enriched by sea spray, and have not yet been corrected for this phenomenon (Keene et al., 1986; Bhatt & McDowell, 2007). After this correction, I will compare this dataset with sediment elemental composition determined by XRF.

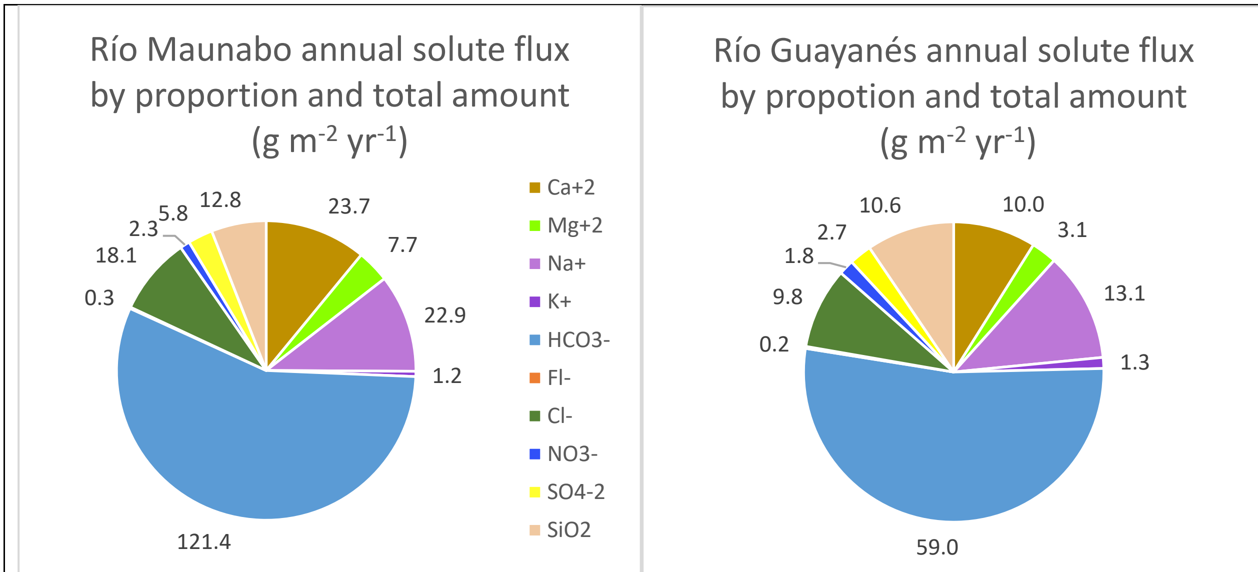

Figure 9a: *watershed solute flux by chemical constituent proportion and annual amount. Annual solute flux for Río Maunabo is 216 g* m^{-2} yr^{-1}*, and 112 g* m^{-2} yr^{-1} *for Río Guayanés.*

Site	Ca^{2+}	Mg^{2+}	Na^{+}	K^{+}	HCO_3^-	Fl^-	Cl^-	NO_3^-	SO_4^{2-}	SiO_2	pH	Dendrogram

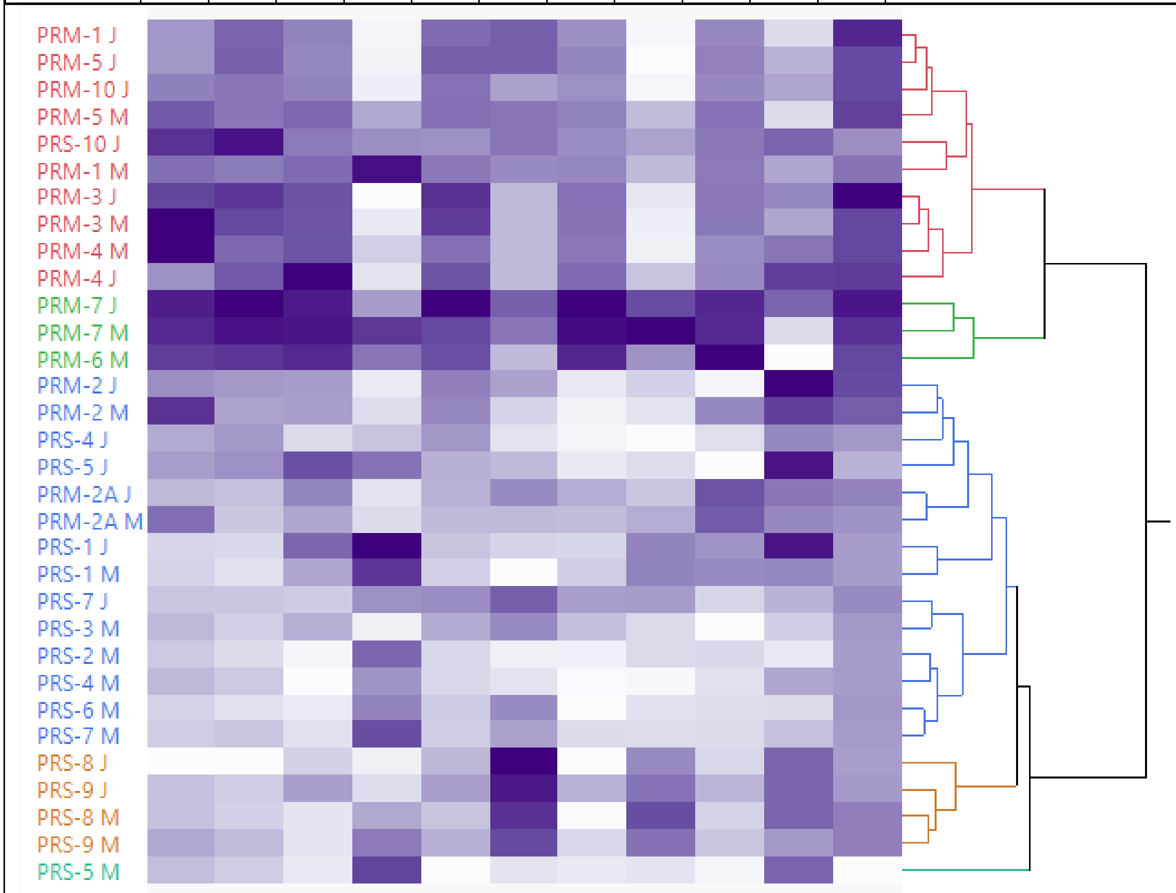

Figure 9b: *hierarchical cluster and color map of water sample geochemistry from both June and March, 2022. June samples end in "J" and March samples end in "M". Sample names (left) are color coded to five hierachical clusters, which are shown in the dendrograph (right). The color map (center) is a visual representation of the concentration of each ion across all measured samples. Shades of purple represent values relative to the measurement range of the given ionic compound, where the highest value in a column is dark purple and the lowest is white. All values were measured in mg/L except pH, which is dimensionless.*

As shown in Figure 9b, several patterns emerge through the comparison of relative dissolved solute flux constituent concentrations. The dendrogram (Figure 9b, right side) provides a visual representation of the relative similarities between samples through the creation of five clusters, shown with different colored lines and sample name text. The largest group of samples (blue) is defined by low overall values relative to those in other groups, particularly Cl^-. The samples in the red group are defined by higher pH, Ca^{2+}, Na^+, and Mg^{2+}, and HCO_3^- values. The orange group is made up of the March and June sample pairs from adjacent sites PRS-8 and PRS-9. This group is characterized by relatively stable concentrations across both sites and seasons, with high Fl^-, and midrange, consistent NO_3^- and SiO_2 values. The green group is comprised of the PRM-7 pair and the March PRM-6 sample, which are again adjacent sample sites. The June PRM-6 sample is missing from this dataset. This group is characterized by the highest overall values, with relatively high concentrations of each ionic compound except SiO_2. The red and green groups suggest proximal and seasonal continuity. The final group is comprised only of PRS-5M. PRS-5J is located in the blue group, demonstrating both discontinuity between seasonal results and between PRS5-M and the rest of the dataset. These preliminary observations will be interesting to compare with results from my upcoming field work to see whether (in)consistencies persist.

I will also use stream bicarbonate concentrations to estimate watershed carbon sequestration through silicate weathering, as one mol of CO_2 is consumed for each mol of bicarbonate measured in solution (Bhatt & McDowell, 2007). Given that these two watersheds have high values of solute flux relative to those measured by Campbell et al. (2022), and more than 50% of that flux is bicarbonate, it will be interesting to see whether these basins are consuming a larger proportion of carbon relative to comparable studies such as Bhatt & McDowell (2007), which was measured in Luquillo, Puerto Rico.

Major cations and anions in stream water and rain geochemistry

Rain chemistry data collected in Luquillo, Puerto Rico between 1983-2010 can contextualize geochemical inputs transported by precipitation (McDowell, 2015; 2017). Luquillo is a mountainous tropical rainforest located roughly 40 km NNE of my field area, with a similarly granitic bedrock lithology. This area is roughly 11 km from the coast, as is my farthest inland sample sites. While these data from Luquillo are imperfectly matched spatially and temporally, they can provide insight about regional rainwater composition. I will use this rainfall geochemistry data to account for and remove sea spray delivered salinity and rainfall delivered ion concentrations from my results to present stream geochemistry that best represents the flux of dissolved load from within my watersheds.

Initial comparisons between the rainwater and sample ionic compositions revealed that while the rainwater pH values were slightly more acidic than the EPA "clean rain" value of 5.6 (EPA, 2022), the river water samples came to an average pH of 8.0. Higher overall ionic compound concentrations in river waters were expected given that the rainwater concentrations ultimately join the flux of ionic compounds mobilized from sediment weathering and soil chemistry processes to make up the river water concentrations.

Sediment composition

While this dataset is not yet complete, the singular PRS (Río Guayanés) sample suggests a distinct elemental composition from the measured PRM (Río Maunabo) samples (Figure 10a, b). PRS-1 contains at least 10% more SiO2 than all of the PRM sites and 5% less AL2O3. This

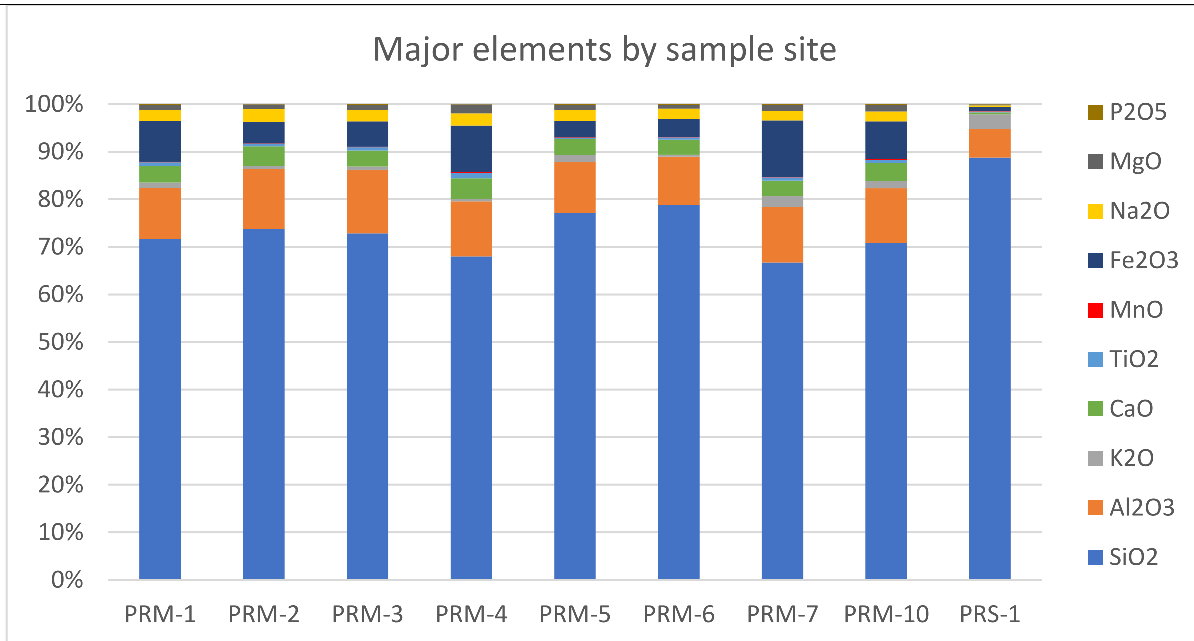

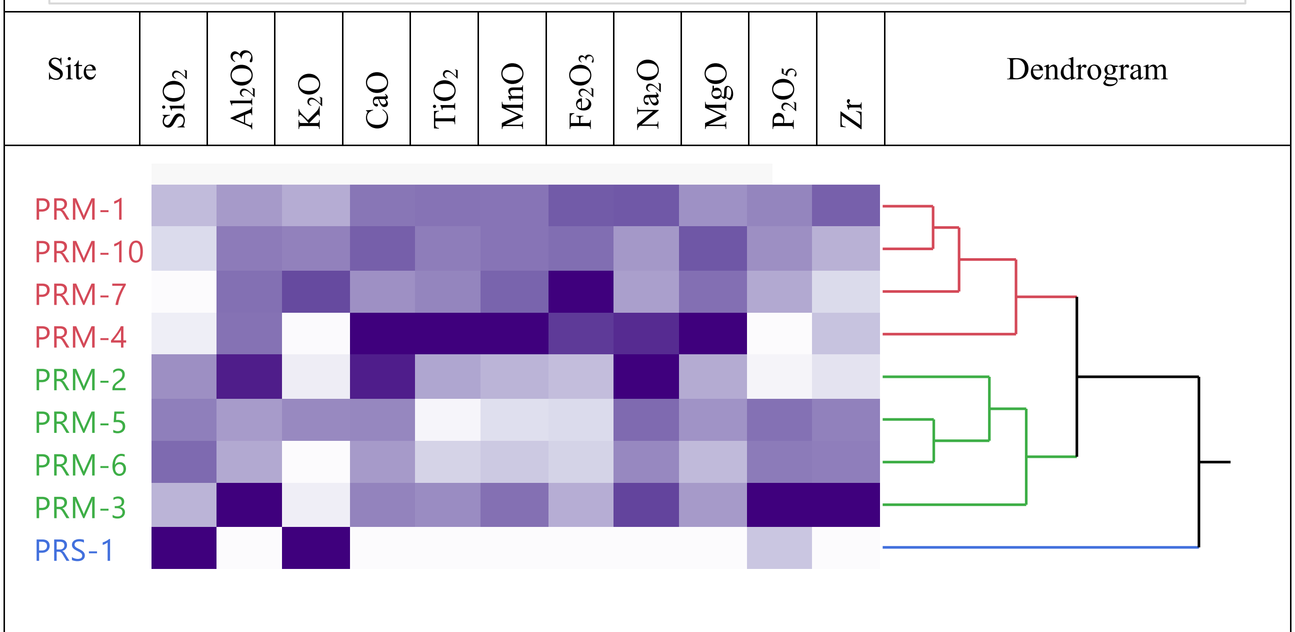

Figure 10a: *Sediment chemical composition by percent. Field site sediment chemical composition by percentage, as determined by XRF analysis.*

Figure 10b*: hierarchical cluster and color map of samples by chemical composition,. Relational analysis of sample composition using hierarchical clustering. Shades of purple represent values relative to the measurement range of the given molecule, where the highest value in a column is dark purple and the lowest is white. All values were measured as a percent of total composition except Zr, which is given in PPM.*

Note: *This data set is not yet complete. It currently contains all eight Río Maunabo (PRM) field sites, and only one site from Río Guayanés (PRS).*

sample is similarly depleted in Fe_2O_3 compared with the samples from Río Maunabo, and to a lesser extent, CaO and Na_2O. Here, the color map of relative chemical constituents is clustered into three groups, though these are less clearly defined than that of the stream water chemistry data (Figure 10b). The dendrogram in this figure again demonstrates the lack of consistency between the PRM and PRS samples within this dataset. It also highlights the composition of PRM-4, which is characterized by low relative K_2O and P_2O_5, and high values for all constituents shown between. Above PRM-4, PRM-1, -10, -7 are characterized by moderate values across the measured constituents, while the samples clustered in the green group lack a clear pattern or consistency.

3.3.4 Ongoing work

While much of my data from this project has already been collected, some analyses are still in progress. Short-lived isotope analysis for the 2022 sediment samples is still ongoing at Oberlin College. The initial results have high levels of uncertainty or suggest concentrations below detection limits. If these measurements are below detection, that will suggest that the sediment measured came from an unmixed layer below 25 cm (the penetration limit of these tracers) (Grande et al., 2021).

I will return to Puerto Rico in June 2023, to resample all 19 field sites, and subsequently conduct all of the sample analyses above on the new samples. By creating two matching, comprehensive data sets collected one year apart, I will be able to evaluate whether there is a disturbance signature in the cosmogenic ^{10}Be concentrations following Hurricane Fiona in September 2022. During this trip, I will reconnect with landowners and community members in this region and continue to mentor undergraduate students. While less structured than the AUGR program, I will train one UVM student, one Oberlin student, and one UVM master's student, in field sampling practices, during this trip. If either undergraduate student is interested, I will welcome continued engagement in this research and/or help to support related undergraduate research projects. Looking ahead, I will prepare the new samples for ^{10}Be extraction in mid October, and compare datasets between 2022 and 2023 as new data is produced. In the meantime, I will complete XRF sample preparation and analysis at Middlebury College, compare these data with short-lived isotope data, conduct GIS basin analysis, and begin to explore spatial relationships between data using GIS during this summer and fall.

4. TIMELINE

Research segment	**Dates**	**Complete?**
Landslide reconstruction project	December 2020 – March 2023	Yes
Educational program design, implementation & documentation	November 2021 – December 2022	Yes
Puerto Rico field reconnaissance & sampling (#1)	March 2022	Yes
Puerto Rico field sampling trip #2 (with AUgR students)	June 2022	Yes
Teaching requirement: NR-195 Perilous Planet Case Studies	August – December 2022	Yes
National conference presentation: Geological Society of America annual meeting, Denver, CO	October 2022	Yes
Dissertation proposal defense	May 15, 2023	No
Comprehensive exams	May 17 – 26, 2023	No
Resampling in Puerto Rico	May 31 – June 6, 2023	No
Finish XRF analysis at Middlebury College	June 2023	No
Complete GIS analysis for PR 2022 data	Summer 2023	No
AUGR student interviews & manuscript completion	Summer 2023	No
New sample prep & Be extraction	Summer – Fall 2023	No
Writing Puerto Rico manuscript	Fall – winter 2023	No
Co-developing Natural Hazards course	Fall – winter 2023	No
Dissertation writing	Fall 2023 – summer 2024	No
Dissertation defense	September 2024	No

**Timeline may be modified to accommodate unexpected opportunities or obstacles*

5. PRODUCTS

5.1 ***Chapter 1:*** *Reconstructing a record of landslides in Burlington, VT*

5.1.1 Bennett, I. B., Bierman, P. R., (2023). A century of urban landslides: the legacy and consequences of altering riverbank landscapes. *(In Review).*

5.1.2 Bennett, I. B., Bierman, P., Halsted, C., "A Century of Urban Landslides: The Legacy and Consequences of Altering Our Landscapes." GSA Annual Meeting, Portland, Oregon, 2021; 04-1 Virtual poster presentation. https://gsa.confex.com/gsa/2021am/webprogram/paper371201.html DOI: 10.1130/Abs/2021am-371201

5.2 ***Chapter 2:*** *Developing an undergraduate training program (AUGR)*
**Denotes AUGR student author*

5.2.1 Bennett, I. B., Bierman, P. R., Soto-Villanueva, K., Sosa Gonzalez, V., Corbett, L. B., "Successes and Challenges in Developing a Program to Engage Underrepresented College Students in Environmental Science Research." (*In preparation).*

5.2.2 Bennett, I. B., Soto-Villanueva, K., Bierman, P., Corbett, L., Acosta-Colon, A., Hughes, K., Whittaker, J., "Inventing AUGR: Reflections on Designing and Implementing an Authentic Undergraduate Geoscience Research Experience." GSA Annual Meeting, Denver, Colorado, 2022; 09-1 Poster presentation. https://gsa.confex.com/gsa/2022am/webprogram/paper381693.html DOI: 10.1130/Abs/2022am-381693

5.2.3 *Mercado-Mercado, A. P,, *Rodriguez-Ramos, I., *Goodwin, J., *Kane, M., *Taylor, B., Bennett, I. B., Bierman P, Corbett, L., Caffee, M., Woodruff, T., Racela, J., Dethier, D., "Water Quality And Erosion Rates Of Landscape Change In Two Watersheds, Southeastern Puerto Rico." GSA Annual Meeting, Denver, Colorado 2022; 09-1 Poster presentation. https://Gsa.Confex.Com/Gsa/2022am/Webprogram/Paper382542.Html DOI: 10.1130/Abs/2022am-382542

5.2.4 *Kane, M., *Rodriguez-Ramos, I., *Mercado-Mercado, A., *Taylor, B., *Goodwin, J., Bennett, I. B., Corbett, L., Bierman, P., Caffee, M., Woodruff, T., "Erosion Rate Analysis Of Two Watersheds In Southeastern Puerto Rico Using 10Be." GSA Annual Meeting, Denver, Colorado, 2022; 09-1 Poster presentation. https://gsa.confex.com/gsa/2022am/webprogram/paper383033.html doi: 10.1130/Abs/2022am-383033

5.2.5 *Taylor B, *Kane M, *Mercado-Mercado A, *Goodwin J, *Rodriguez-Ramos I, Bennett, I. B., Bierman P, Racela J, Dethier D. "Cracking the Dissolved Inorganic Materials Code: Comparing Two Puerto Rico Rivers Across Seasons." GSA Annual meeting, Denver, Colorado; 09-1 Poster presentation. https://gsa.confex.com/gsa/2022AM/webprogram/Paper382951.html DOI: 10.1130/abs/2022AM-382951

5.2.6 *Goodwin, J., *Rodriguez-Ramos, I., *Taylor, B., *Mercado-mercado, A., *Kane, M., Bennett, I. B., Perdrial, J., Bierman, P., "Evaluating E. coli, Dissolved Organic Carbon, and Total Dissolved Nitrogen Within two Southeastern Puerto Rico Watersheds." GSA Connects 2022 meeting in Denver, Colorado; 09-1 Poster abstract, student could not attend conference. https://gsa.confex.com/gsa/2022AM/webprogram/Paper382818.html DOI: 10.1130/abs/2022AM-382818

5.2.7 Successful grant writing experiences: 1) https://www.colorado.edu/program/agesgeochronology/ages-dig 2) https://www.uvm.edu/news/gund/gund-institute-awards-inaugural-equity-and-justice-grants

5.2.8 RSENR News coverage: https://www.uvm.edu/news/rsenr/uvm-student-project-seeks-diversify-stem

6. REFERENCES

Adetunji, O. O., Ba, J. C. M., Ghebreab, W., Joseph, J. F., Mayer, L. P., & Levine, R. (2012). Geosciences Awareness Program: A program for broadening participation of students in Geosciences. *Journal of Geoscience Education*, *60*(3), 234–240. https://doi.org/10.5408/10-208.1

Aquagenx (n.d.) CBT EC+TC Kit: Portable Quality Test Kits for P/A and MPN Test Results. Retrieved from: https://www.aquagenx.com/dilutions-cbt-ectc/

Baber, L. D., Pifer, M. J., Colbeck, C., & Furman, T. (2010). Increasing diversity in the geosciences: Recruitment programs and student self-efficacy. *Journal of Geoscience Education*, *58*(1), 32–42. https://doi.org/10.5408/1.3544292

Balco, G., (2017). "The online erosion rate calculator formerly known as the CRONUS-Earth online erosion rate calculator:" V. 3. https://hess.ess.washington.edu/math/v3/v3_erosion_in.html

Bawiec, Walter J., 1998, Geology, geochemistry, geophysics, mineral occurrences, and mineral resource assessment for the commonwealth of Puerto Rico: Open-File Report 98-38, U.S. Geological Survey, Reston, Virginia. Retrieved from: https://mrdata.usgs.gov/geology/pr/map-pr.html#home

Berhe, A. A., Barnes, R. T., Hastings, M. G., Mattheis, A., Schneider, B., Williams, B. M., & Marín-Spiotta, E. (2022). Scientists from historically excluded groups face a hostile obstacle course. *Nature Geoscience*, *15*(1), 2–4. https://doi.org/10.1038/s41561-021-00868-0

Bernard, M. A. (2020). *The Importance of Science Identity for Inclusion*. National Institutes of Health Blog. https://diversity.nih.gov/blog/2020-12-04-importance-science-identity-inclusion#:~:text=What is Science Identity%3F,contexts %5B1%2C 2%5D.

Bienroth, F. H. (1969). An Outline of the Geology of Puerto Rico. University of Puerto Rico Mayaguez Campus. Agricultural Experiment Station Rio Piedras, Puerto Rico. Retrieved from: https://www.uprm.edu/tamuk/wp-content/uploads/sites/299/2019/07/Outline_Geology_PR_1969.pdf

Bierman P. R., et al. (2020) ¡Cuba! River water chemistry reveals rapid chemical weathering, the echo of uplift, and the promise of more sustainable agriculture. GSA TODAY. doi.org/10.1130/GSATG419A.1

Bierman, P. R., Larsen, J. (2008a). Laboratory Safety Manual: Rock and Sediment Mineral Preparation *UVM/NSF Community Cosmogenic Facility.* Retrieved from: https://www.uvm.edu/cosmolab/methods.html

Bierman, P. R., Larsen, J. (2008b). Quartz Purification Protocol. *UVM/NSF Community Cosmogenic Facility.* Retrieved from: https://www.uvm.edu/cosmolab/methods.html

Bierman, P. R., Lini, A., Zehfuss, P., Church, A., Thompson, P. D., Southon, J., Baldwin, L., (1997). Postglacial Ponds and Alluvial Fans: Recorders of Holocene Landscape History. *GSA Today.* Retrieved from: https://www.uvm.edu/cosmolab/papers/Bierman_1997_1155.pdf

Bierman, P. R., & Steig, E. (1996). Estimating rates of denudation and sediment transport using cosmogenic isotope abundances in sediment. *Earth Surface Processes and Landforms*, *21*(2), 125–139. doi.org/10.1002/(SICI)1096-9837(199602)21:2%3C125::AID-ESP511%3E3.0.CO;2-8

Bierman, P. R., Lini, A., Davis, P. T., Southon, J., Baldwin, L., Church, A. and Zehfuss, P. (1997) Post-glacial ponds and alluvial fans: recorders of Holocene landscape history. GSA Today. v. 7, p. 1-8.

Bhatt, M. P., McDowell, W. H., (2007). Controls on major solutes within the drainage network of a rapidly weathering tropical watershed. *Water Resources Research 43.* doi:10.1029/2007WR005915

Brocard, G. Y., Willenbring, J. K., Scatena, F. N., Johnson, A. H., (2015). Effects of a tectonically-triggered wave of incision on riverine exports and soil mineralogy in the Luquillo Mountains of Puerto Rico. *Applied Geochemistry.* 63. 586-598. https://doi.org/10.1016/j.apgeochem.2015.04.001

Brown, E.T., Stallard, R.F., Larsen, M.C., Raisbeck, G.M., Yiou, F., (1995). Denudation rates determined from the accumulation of in situ produced 10Be in the Luquillo Experimental Forest, Puerto Rico, Earth Planet. Sci. Lett. 129. 193–202.

Brown, E.T., Stallard, R.F., Larsen, M.C., Bourlès, D.L., Raisbeck, G.M., Yiou, F., (1998). Determination of predevelopment denudation rates of an agricultural watershed (Cayaguas River, Puerto Rico) using in-situ-produced 10Be in river-borne quartz, Earth Planet. Sci. Lett. 160. 723–728.

Bruthers, C. B., & Matyas, M. L. (2020). Undergraduates from underrepresented groups gain research skills and career aspirations through summer research fellowship. *Advances in Physiology Education*, *44*(4), 525–539. https://doi.org/10.1152/advan.00014.2020

Caban, P., (2005). Puerto Rico, Colonialism In. Latin American, Caribbean, and U.S. Latino Studies Faculty Scholarship. 19. https://scholarsarchive.library.albany.edu/lacs_fac_scholar/19

Callahan, C. N., LaDue, N. D., Baber, L. D., Sexton, J., van der Hoeven Kraft, K. J., & Zamani-Gallaher, E. M. (2017). Theoretical perspectives on increasing recruitment and retention of underrepresented students in the geosciences. *Journal of Geoscience Education*, *65*(4), 563–576. https://doi.org/10.5408/16-238.1

Campbell, M.K. et al., (2022). Cosmogenic nuclide and solute flux data from central Cuba emphasize the importance of both physical and chemical denudation in highly weathered landscapes: Geochronology Discussions, v. 2021, p. 1–29, doi:10.5194/gchron-2021-31.

Carey, J. M., Cosgrove, B., Norton, K., Massey, C. I., Petley, D. N., Lyndsell, B., (2021). Debris flow-slide initiation mechanisms in fill slopes, Wellington, New Zealand. *Landslides. 18*. 2016-2072. https://link.springer.com/article/10.1007/s10346-021-01624-6

Cheadle, M., (2015). The Tectonic Setting and Geology of Puerto Rico and its Surrounding Seafloor. *NOAA Ocean Exploration.* Retrieved from: https://oceanexplorer.noaa.gov/okeanos/explorations/ex1502/background/geology/welcome.html

Clague, J. J., Stead, D., Eds. (2012). Landslides: Types, Mechanisms and Modeling. Cambridge University Press.

Cohen, D., Schwarz, M. (2017) Tree-root control of shallow landslides. EGU Earth Surface Dynamics., 5, 451-477. https://doi.org/10.5194/esurf-5-451-2017

Corbett, L. B., Bierman, P. R., Rood, D. H., (2016). An approach for optimizing *in-situ* cosmogenic ^{10}Be sample preparation. *Quaternary Geochronology.* 33. 24-34. https://doi.org/10.1016/j.quageo.2016.02.001

Du, J. Z., Zhang, J., Baskaran, M. (2011). Applications of Short-Lived Radionuclides (7Be, 210Pb, 210Po, 137Cs and 234Th) to Trace the Sources, Transport Pathways and Deposition of Particles/Sediments in Rivers, Estuaries and Coasts. *Handbook of Environmental Isotope Geochemistry, Natural and Anthropogenic Cd Isotope Variations. 1.* 305-329. Springer Heidelberg Dordrecht London New York. DOI 10.1007/ 978-3-642-10637-8

Dunai, T.J., (2010). Cosmogenic Nuclides: Principles, Concepts and Applications in the Earth Surface Sciences: Cambridge, Great Britain, Cambridge University Press, www.cambridge.org/9780521873802.

Dutt, K., (2020). Race and racism in the geosciences. *Nature Geoscience. 13*(1) 2-3. https://doi.org/10.1038/s41561-019-0519-z

Earle, S. (2015). Physical Geology. “Mechanical Weathering.” *BCcampus Open Education*. Retrieved from: https://opentextbc.ca/geology/chapter/5-1-mechanical-weathering/

EPA. (2022). What is Acid Rain? *United States Environmental Protection Agency.* Retrieved from: https://www.epa.gov/acidrain/what-acid-rain.

Fastest Growing Occupations. (2022). U.S. Bureau of Labor Statistics Occupational Outlook Handbook. https://www.bls.gov/ooh/fastest-growing.htm

Fisk, J. J. P. (2022). Speaking of Abundance: Taíno Ecolinguistic Ontologies, Pre-colonial Biocultural Systems, and Decolonial Pathways to Food and Material Sovereignty in Puerto Rico. *University of Hawai'I Manoa Dissertations Publishing.* Retrieved from: https://www.proquest.com/openview/c54cf538b966c9e5f2eda31b31809013/1?pq-origsite=gscholar&cbl=18750&diss=y

Fleming R. W., Taylor, F. A., Estimating the Costs of Landslide Damage in the United States. United States Department of the Interior. Geological Survey Circular 832. (1980). https://pubs.usgs.gov/circ/1980/0832/report.pdf

Follmer, D. J., Zappe, S., Gomez, E., & Kumar, M. (2017). Student Outcomes from Undergraduate Research Programs: Comparing Models of Research Experiences for Undergraduates (REUs). *Scholarship and Practice of Undergraduate Research*, *1*(1), 20–27. https://doi.org/10.18833/spur/1/1/5

Foster, M. A., Anderson, R. S. (2016). Assessing the effect of a major storm on 10BE concentrations and inferred basin-averaged denudation rates. Quarternary Geochronology. 34. 58-68. http://dx.doi.org/10.1016/j.quageo.2016.03.006

Galarza, N., (2015). Greening a Drug-Addicted Economy: Can Puerto Rico Ease Away from the Toxic Pharmaceutical Industry to a Sustainably Diverse Economy? Student Theses 2015-Present. 17. https://fordham.bepress.com/environ_2015/17

Grande, A., Schmidt, A. H., Bierman, P. R., Corbett, L. B., Lóped-Lloreda, C., Willenbring, J., McDowell, W. H., Caffee, M. W., (2021). Landslides, hurricanes, and sediment sourcing impact basin-scale erosion estimates in Luquillo, Puerto Rico. *Earth and Planetary Science Letters.* 562. https://doi.org/10.1016/j.epsl.2021.116821

Granger, D. E., Kirchner, J. W., & Finkel, R. (1996). Spatially Averaged Long-Term Erosion Rates Measured from in Situ-Produced Cosmogenic Nuclides in Alluvial Sediment. *The Journal of Geology*, *104*(3), 249–257. https://www.jstor.org/stable/30068190

Harden, C. P., Chin, A., English, M. R., Fu, R., Galvin, K. A., Gerlak, A. K., McDowell P. F., McNamara, D. E., Peterson J. M., Poff, N. L., Rosa, E. A., Solecki, W. D., Wohl, E. E., (2014). Understanding Human-Landscape Interactions in the "Anthropocene". *Environmental Management.* 53. 4-13. DOI 10.1007/s00267-013-0082-0

Highland, L. M., Bobrowsky, P., (2008). The Landslide Handbook – A Guide to Understanding Landslides. United States Geological Survey, Circular 1325. Retrieved from: https://pubs.usgs.gov/circ/1325/

Howard, A. (University of V. (2022, October). UVM Student Project Seeks to Diversify STEM. *Rubenstein School of Environment and Natural Resources News & Events*. https://www.uvm.edu/news/rsenr/uvm-student-project-seeks-diversify-stem

Huntoon, J. E., & Lane, M. J. (2007). Diversity in the geosciences and successful strategies for increasing diversity. *Journal of Geoscience Education*, *55*(6), 447–457. https://doi.org/10.5408/1089-9995-55.6.447

Jack, A. A. (2019). *The Privileged Poor*. Harvard University Press. https://anthonyabrahamjack.com/

Johnston, E. C., Davenport, F. V., Wang, L., Caers, J. K., Muthurkishnan, S., Burke, M., Diffenbaugh, N. S. (2021). American Geophysical Union. Geophysical Research Letters. 10.1029/2021GL094038 Quantifying the Effect of Precipitation on Landslide Hazard in Urbanized and Non-Urbanized Areas (wiley.com)

Keene, W. C., A. A. P. Pszenny, J. N. Galloway, and M. E. Hawley (1986), Sea-salt corrections and interpretation of constituent ratios in marine precipitation, *J. Geophys. Res.,* 91(D6), 6647–6658.

Knight, A., (2022). Diversity in Geochronology: "Best Practices for Recruitment and Retention." Presentation, 2022 AGeS Workshop, Boulder, CO. https://www.colorado.edu/program/agesgeochronology/sites/default/files/attached-files/Knight_Diversity%20in%20Geochronology_%20Best%20Practices%20for%20Recruitment%20and%20Retention_2022AGeSWorkshop.pdf

Kohl, C. P., Nishiizumi, K. (1992). Chemical isolation of quartz for measurement of in-situ -produced cosmogenic nuclides. *Geochimica et Cosmochimica Acta. 56*(9). 3583-3587. https://doi.org/10.1016/0016-7037(92)90401-4

Krushensky, R. D. (2000). Geology of the Island of Puerto Rico between 66 7' 30" and 66 52' 30" West Longitude at a Scale of 1:100,000. Map. U.S Geological Survey Open-File Report. USGS OFR 98-38. Reston, Virginia. http://pubs.usgs.gov/of/1998/of98-038/.

Kurtz, A., Lugolobi, F., Salvucci, G., (2011). Germanium-silicon as a flow path tracer: Application to the Rio Icacos watershed. *Water Resources Research. 47*. Doi:10.1029/2010WR009853

Lacasse. S., Nadim F., (2009). Landslide Risk Assessment and Mitigation strategy. K. Sassa & P. Canuti (Eds.), *Landslides: Disaster Risk Reduction*. (pp. 31-61) Springe, Berlin, Heidelberg. https://doi.org/10.1007/978-3-540-69970-5_3

Lal, D. (1991). Cosmic ray labeling of erosion surfaces: in situ nuclide production rates and erosion models. *Earth and Planetary Science Letters. 104*(2-4), 424-439. https://doi.org/10.1016/0012-821X(91)90220-C

Lal, D., Peters, B. (1967). Cosmic Ray Produced Radioactivity on the Earth. In: Sitte, K. (eds) Kosmische Strahlung II / Cosmic Rays II. Handbuch der Physik / Encyclopedia of Physics, vol 9 / 46 / 2. Springer, Berlin, Heidelberg. https://doi.org/10.1007/978-3-642-46079-1_7

Lara, M. C., Buss, H., Pogge, P., Von Strandmann et al., (2017). The influence of critical zone processes on the Mg isotope budget in a tropical, highly weathered andesitic catchment. *Geochimica et Cosmochimica Acta. 202.* 77-100. 10.1016/j.gca.2016.12.032

Levine, R., González, R., Cole, S., Fuhrman, M., & le Floch, K. C. (2007). The geoscience pipeline: A conceptual framework. *Journal of Geoscience Education*, *55*(6), 458–468. https://doi.org/10.5408/1089-9995-55.6.458

Lévy, S., Jaboyedoff, M., Locat, J., Demers, D., (2012). Erosion and channel change as factors of landslides and valley formation in Champlain Sea Clays: The Chacoura River, Quebec, Canada. Geomorphology. Volumes 145–146. Pages 12-18. ISSN 0169-555X. https://doi.org/10.1016/j.geomorph.2011.09.014.

MacLeod, A., Hofmeister, R. J., Wang, Y., Burns, S., Landslide Indirect Losses: Methods and Case Studies from Oregon. Department of Geology and Mineral Industries. (2005). Retrieved from: https://citeseerx.ist.psu.edu/viewdoc/download?doi=10.1.1.485.4605&rep=rep1&type=pdf

Marrero, A., Tamez, M., Rodriguez-Orengo, J. F., Mattei, J. (2021). The association between purchasing locally produced food and diet quality among adults in Puerto Rico. *Public Health Nutr. 24*(13): 4177-4186. DOI:10.1017/S1368980020003134

McDowell, W. H., (2015). Chemistry of rainfall and throughfall from El Verde and Bisley. LTER Network Retrieved from: https://search.dataone.org/view/https%3A%2F%2Fpasta.lternet.edu%2Fpackage%2Fmetadata%2Feml%2Fknb-lter-luq%2F174%2F2110731. Metadata: https://pasta.lternet.edu/package/metadata/eml/knb-lter-luq/174/2110731

McDowell, W. H., (2017). Chemistry of stream water from the Luquillo Mountains ver 4923051. Environmental Data Initiative. https://doi.org/10.6073/pasta/f9df56348f510da0113b1e6012fa2967 (Accessed 2024-05-22).

Monroe, W. H. (1980). Some Tropical Landforms of Puerto Rico. Geological Survey Professional Paper 1159, United States Department of the Interior. *United States Government Printing Office, Washington.* Retrieved from: https://pubs.usgs.gov/pp/1159/report.pdf

Montgomery, D. R., Schmidt, K. M., Greenberg, H. M., Deitrich, W. E. (2000). Forest clearing and regional landsliding. Geology. 28 (4): 311-314. https://doi.org/10.1130/0091-7613(2000)28<311:FCARL>2.0.CO;2

Moore, O., Buss, H., Dosseto, A., (2019). Incipient chemical weathering at bedrock fracture interfaces in a tropical critical zone system, Puerto Rico. *Geochimica et Cosmochimica Act. 252. 61-87. https://doi.org/10.1016/j.gca.2019.02.028*

NWS. (n.d.) National Weather Service. Puerto Rico Local Data/Records. “Mean Annual Rainfall 1981 – 2010: Puerto Rico.” *National Oceanic and Atmospheric Administration.* Retrieved from: https://www.weather.gov/images/sju/hydrology/2010_ncdc_precip_normals_PR_USVI.jpg

O'Connell, S., & Holmes, M. A. (2011). Obstacles to the recruitment of minorities into the geosciences: A call to action. *GSA Today*, *21*(6), 52–54. https://doi.org/10.1130/G105GW.1

Pearson, A. R., & Schuldt, J. P. (2014). Facing the diversity crisis in climate science. *Nature Climate Change*. *4*(12), 1039–1042. https://doi.org/10.1038/nclimate2415

Perdrial, J., Thompson, A., Chorover, J. (2015). "Soil Geochemistry in the Critical Zone: Influence on Atmosphere, Surface- and Groundwater Composition." Principals and Dynamics of the Critical Zone, edited by Giardino, J. R., Houser, C., *Developments in Earth Surface Processes. 19.* 173-201. DOI: 10.1016/B978-0-444-63369-9.00006-9

Perkins, J. P., Reid, M. E., Schmidt, K. M. (2017). Control of landslide volume and hazard by glacial stratigraphic architecture, northwest Washington State, USA. Geology. 45 (12) 1139 – 1142. https://doi.org/10.1130/G39691.1

Portenga, E. W., Bierman, P. R. (2011). Understanding earth's eroding surface with 10Be. *GSA Today. 21*(8). 4-10. DOI: 10.1130/G111A.1

Quartz Purity Testing. (2013). *UVM/NSF Community Cosmogenic Facility.* Retrieved from: https://www.uvm.edu/cosmolab/methods.html

Quock M., Schmidt, A. H., Corbett, L. B., Bierman, P. R., Hidy, A. J., Caffee, M. (2021). Hurricanes alter 10Be concentrations in tropical river sediment but do not change regional erosion rate estimates. *Earth Surface Processes and Landforms.* 1-16. DOI: 10.1002/esp.5310

Regmi, N. R., Giardino, J. R., McDonald, E. V., Vitek, J. D., A comparison of logistic regression-based models of susceptibility to landslides in western Colorado, USA. Landslides (2014). 11:247-262. DOI 10.1007/s10346-012-0380-2. Retrieved from: https://link.springer.com/content/pdf/10.1007/s10346-012-0380-2.pdf

Riebe, C. S., Granger, D. E., (2013). Quantifying effects of deep and near-surface chemical erosion on cosmogenic nuclides in soils, saprolite, and sediment. *Earth Surface Processes and Landforms. 38*(5) 523-533. DOI: 10.1002/esp.3339

Riebe, C. S., Kirchner, J. W., Granger, D. E., (2001). Quantifying quartz enrichment and its consequences for cosmogenic measurements of erosion rates from alluvial sediment and regolith. *Geomorphology. 40*(1-2) 15-19. Retrieved from: https://www.sciencedirect.com/science/article/abs/pii/S0169555X01000319

Roman, T., & Logue, E. (2012). Academic factors that affect undergraduate research experiences. *Journal of Educational Psychology*, *104*(2), 499–514. https://doi.org/https://doi.org/10.1037/a0026851

Runkle, J., K.E. Kunkel, S.M. Champion, L.-A. Dupigny-Giroux, and J. Spaccio, 2022: Vermont State Climate Summary 2022. NOAA Technical Report NESDIS 150-VT. NOAA/NESDIS, Silver Spring, MD, 4 pp. https://statesummaries.ncics.org/chapter/vt/

Sargent, J. F. (2014). The U.S. Science and engineering workforce: Recent, current, and projected employment, wages, and unemployment. *The U.S. Science and Engineering Workforce: Employment and Wage Trends*, 1–47.

Schimmer, R., (n.d.) *Puerto Rico Case Study: Colonial Genocides.* Yale University Genocide Studies Program. Retrieved from: https://gsp.yale.edu/case-studies/colonial-genocides-project/puerto-rico.

Singleton, A. A., Schmidt, A. H., Bierman, P. B., Rood, D. H., Neilson, T. B., Greene, E. S., Bower, J. A., Perdrial, N. (2016). Effects of grain size, mineralogy, and acid-extractable grain coatings on the distribution of the fallout radionuclides 7Be, 10Be, 137Cs, and 210Pb in river sediment. *Geochimica et Cosmochimica Acta. 197.* 71-86. http://dx.doi.org/10.1016/j.gca.2016.10.007

Stern, P. C. (1993). A Second Environmental Science: Human-Environment Interactions. *Science. 260*(5116). DOI: 10.1126/science.260.5116.1897. Retrieved from: https://www.science.org/doi/pdf/10.1126/science.260.5116.1897?casa_token=A5HgXPD1GnkAAAAA:Zeq2P0eVJb_Zd-MvPRqEUGl_qJ6_UjAgdhj81bddg4VMxn-9kwvEEkwm4rDKdNiuhM0Trv1NFcg4P3g

Stallard, R., (1988). Weathering and Erosion in the Humid Tropics. *Environmental Science, Geology*. DOI:10.1007/978-94-009-3071-1_11. Retrieved from: https://www.semanticscholar.org/paper/WEATHERING-AND-EROSION-IN-THE-HUMID-TROPICS-Stallard/ae38591cf76c703b32c416fb029dcf2d1adb9110

Taylor, D. E. (2018). Racial and ethnic differences in the students' readiness, identity, perceptions of institutional diversity, and desire to join the environmental workforce. *Journal of Environmental Studies and Sciences*, *8*(2), 152–168. https://doi.org/10.1007/s13412-017-0447-4

U.S. Census Bureau (n.d.) *Quick Facts: Puerto Rico.* Retrieved from: https://www.census.gov/quickfacts/fact/table/PR/IPE120221

USDA (2017). 2017 Census of Agriculture Highlights: Puerto Rico Agriculture. Census of Agriculture Historical Archive. https://www.nass.usda.gov/AgCensus/

USDA (1987). 1987 Census of Agriculture: Geographic Area Series: Puerto Rico. Census of Agriculture Historical Archive. https://agcensus.library.cornell.edu/census_parts/1987-puerto-rico/

USDA (1964). Number and Area of Farms: 1910 to 1964: Statistics for Puerto Rico. Census of Agriculture Historical Archive. https://agcensus.library.cornell.edu/census_parts/1987-puerto-rico/

USGS (n.d.). Groundwater Atlas of the United States Alaska, Hawaii, Puerto Rico and the US Virgin Islands HA 730-N. *United States Geological Survey.* Retrieved from: https://pubs.usgs.gov/ha/ha730/ch_n/N-PR_VItext1.html

USGS (May, 2023a). Rio Maunabo at Lizas, PR - 50090500. Data. *Discharge, cubic feet per second.* Retrieved from: https://waterdata.usgs.gov/monitoring-location/50090500/#parameterCode=00065&period=P7D

USGS (May, 2023b). Rio Guayanes NR Yabucoa, PR – 50083500. Data. *Discharge, cubic feet per second.* Retrieved from: https://waterdata.usgs.gov/monitoring-location/50083500/#parameterCode=00065&period=P7D

UVM Cosmogenic Laboratory: Be/Al Extraction. (2018). *UVM/NSF Community Cosmogenic Facility.* Retrieved from: https://www.uvm.edu/cosmolab/methods.html

Van Westen, C. J., Rengers, N., Soeters, R., (2003). *Use of Geomorphological Information in Landslide Susceptibility Assessment*. Natural Hazards 30. P. 399-419

Wallemacq, Pascaline & UNISDR, & CRED,. (2018). *Economic Losses, Poverty and Disasters 1998-2017*. 10.13140/RG.2.2.35610.08643. Retrieved from: https://www.researchgate.net/publication/331642958_Economic_Losses_Poverty_and_Disasters_1998-2017/citation/download

Whittaker, J. A., & Montgomery, B. L. (2012). Cultivating diversity and competency in STEM: Challenges and remedies for removing virtual barriers to constructing diverse higher education communities of success. *Journal of Undergraduate Neuroscience Education*, *11*(1), 44–51.

White, A., Blum, A., Schultz, M., et al., (1998). Chemical weathering in a tropical watershed, Luquillo Mountains, Puerto Rico: I. Long-term versus short-term weathering fluxes. *Geochimica et Cosmochimica Acta*, *62*(2), 209–226.

Wolfe, B. A., & Riggs, E. M. (2017). Macrosystem analysis of programs and strategies to increase underrepresented populations in the geosciences. *Journal of Geoscience Education*, *65*(4), 577–593. https://doi.org/10.5408/17-256.1

8. APPENDIX

Table 1: *Chronological list of all known landslides along Riverside Avenue as of March 2023*

Slide	Year	Date	Size information	Location & Notes	Repair Cost	Cause	Source(s)
1	1952	Spring	Unknown; "[Took] away sizable portions of the pavement."	Near Fairview garage (114 Riverside Ave). Prompts 1953 winter street project.	Unknown	Unknown	("Mild Winter" 1953)
2	1955	August 17	Unknown; "The water took away much fill underneath the [side]walk."	Just east of 239 Riverside Avenue. "Washout Wednesday."	Unknown	2.37 inch rain storm on August 17 caused flooding, drainage problems across city.	("Storm is worst" 1955; "City Light" 1955)
3	1955	End of August	Unknown; Articles suggests multiple washouts along Riverside Ave following storm.	Occurred 1km from the intersection with N. Winooski Avenue. Across from Fairview Garage (114 Riverside Ave).	$37,500	Unknown	("Burlington Youths " 1955' "Washout Rips Riverside" 1955; "St. Johnsbury" 1955)
4	1955	September 6	A section of road and sidewalk slid down the embankment, creating a 7 m x 15 m hole in the road and breaking a water main.	Same location as slide #3, which had just been patched. Across from Fairview Garage (114 Riverside Ave).	$35,000	Unknown	("Burlington " 1955; "Washout Rips Riverside" 1955)
5	1955	November 18	Thousands of yards of fill.	Across from Hillside Terrace Development. Composed of fill, half dozen big pine trees.	Unknown	Potentially the excavation for a new culvert along the bank of the old washout.	("Washout Rips Riverside" 1955; Detore Collection 1955, Landscape Change Program)
6	1958	March 31	Unknown	Within 10 ft of sidewalk, caused it to drop "some". Across from Fairview garage (114 Riverside Ave), same location as September 6, 1955 slide.	Cost of 5,000 cubic yards of rock fill required to stabilize bank.	"Underground water seepage that undermines the fill" and inadequate drainage.	("Small Landslide" 1958; "Crews Begin" 1958)
7	1968	May 9	"Tons of earth and junked cars…"	389 Riverside Ave; came within 15 ft of road.	Unknown	Occurred after fill was dumped.	("Landslide Threatens" 1968)
8	1968	July 1	Unknown	Location unknown. Caused cars to fall into river; stabilized with "tons of crushed stone."	Unknown	Unknown	("Firm Foundation" 1968)

9	1972	Before August 29	Unknown; right above the Winooski Salmon Hole.	Minimal information available, images show an undermined sidewalk and road.	Unknown	Unknown	Landscape Change Program images LS57951-LS57954
10	1974	Early February	Unknown; large enough that material entering the Winooski River altered its flow.	Across from the Winooski Sewage treatment plant. Concern that it might change the course of the Winooski River by altering its bed.	Unknown	Unknown	(Wolff 1974)
11	1976	September	Article estimated 4,000 yards of material; caused increased scouring of the riverbanks.	"Occurred about 35 ft from Riverside Avenue near B.J.'s Variety Market." (454 Riverside Ave).	Estimate: $45,000	"May have been caused by heavy rains in August and September, and resulting high river levels which undercut the supporting banks."	("Mudslide cleanup" 1977; "Landslide Repair" 1976)
12	1981	June 12	12 m across, "Several thousand cubic yards" that "partially blocked" the Winooski.	Across from Koffee Kup Bakery (436 Riverside Ave). Mayor requested $350,000 to stabilize.	Work in 1983 cost between $80,000-$100,000.	Illegal dumping of landfill material on private property.	("Workers Begin" 1983; "Debris Slides" 1981; Reilly 1981; "Dismissal requested" 1981)
13	1983	Unknown	"[The property owner] told the board he has lost 20 feet of land in the last year."	Undermined the Riverside Glass and Mirror Inc building (463 Riverside Ave) "The back of that building is handing in the air over the eroding bank."	$5,000 to hire a consultant. "Shoring up the entire problem area, which extends from the Winooski Bridge to Intervale Road… Would cost hundreds of thousands of dollars."	Potentially caused by illegal dumping; determined that it was not caused by drainage issues.	(Melvin 1983)
14	1989	Fall	Unknown	Within the Salmon Run apartments construction area (220 Riverside Ave)	Unknown	Trees were cut for development, destabilizing the slope.	("Ward 1" 1990)
15	1998	Unknown	Unspecified; Visual estimate: 15 m wide by 7 m deep	Undermined the Riverside Glass and Mirror Inc building at 463 Riverside Ave.	Unknown	Attributed to "underground water problem"	("Retail Roundup" 1998; Melvin 1983).

16	2007	Unknown; prior to inspection on July 12	Unknown	Undermined single bedroom house at 389B Riverside Avenue	Unknown	Unknown	(Department of Planning and Zoning 2008)
17	2019	October 31	3600-5000m^3; more than 36 m wide at the top of the scarp	385 Riverside Ave; Just west of Hall's Hitches & Welding.	Unknown	3.3 inches of rain in 6-10 hours exacerbated slope instability caused by illegal dumping	(Baird 2019; Hastings & Taber n.d.; Google Earth 2023)
18	2019	October 31	24 m wide at the top of the scarp	Two landslides (smaller than #17) occurred on either side of the Burlington Collision Center (411 Riverside Ave)	Unknown	3.3 inches of rain in 6-10 hours exacerbated slope instability caused by illegal dumping	(Hastings & Taber n.d.; Google Earth 2023)

Caption: *Comprehensive list of landslide events along Riverside Avenue, in Burlington, Vermont, to date. We compiled this information primarily from Burlington Free Press Newspaper archives and photography accessible from the Vermont Landscape Change Program. The Burlington Free Press uses Imperial or United States Customary Units, while we use metric units in our measurements.*